

Flavor Changing Neutral Currents involving Heavy Quarks with Four Generations

Abdesslam Arhrib^{1,2} and Wei-Shu Hou³

¹National Center for Theoretical Sciences, PO-Box 2-131 Hsinchu, Taiwan 300

²Faculté des Sciences et Techniques B.P 416 Tangier, Morocco

³Department of Physics, National Taiwan University, Taipei, Taiwan 106

Abstract

We study various flavor changing neutral currents (FCNC) involving heavy quarks in the Standard Model (SM) with a sequential fourth generation. After imposing $B \rightarrow X_s \gamma$, $B \rightarrow X_s l^+ l^-$ and $Z \rightarrow b \bar{b}$ constraints, we find $\mathcal{B}(Z \rightarrow s \bar{b} + \bar{s} b)$ can be enhanced by an order of magnitude to 10^{-7} , while $t \rightarrow cZ, cH$ decays can reach 10^{-6} , which are orders of magnitude higher than three generation SM. However, these rates are still not observable for the near future. With the era of Large Hadron Collider approaching, we focus on FCNC decays involving fourth generation b' and t' quarks. We calculate the rates for loop induced FCNC decays $b' \rightarrow bZ, bH, bg, b\gamma$, as well as $t' \rightarrow tZ, tH, tg, t\gamma$. If $|V_{cb'}|$ is of order $|V_{cb}| \simeq 0.04$, tree level $b' \rightarrow cW$ decay would dominate, posing a challenge since b -tagging is less effective. For $|V_{cb'}| \ll |V_{cb}|$, $b' \rightarrow tW$ would tend to dominate, while $b' \rightarrow t'W^*$ could also open for heavier b' , leading to the possibility of quadruple- W signals via $b'\bar{b}' \rightarrow b\bar{b}W^+W^-W^+W^-$. The FCNC $b' \rightarrow bZ, bH$ decays could still dominate if $m_{b'}$ is just above 200 GeV. For the case of t' , in general $t' \rightarrow bW$ would be dominant, hence it behaves like a heavy top. For both b' and t' , except for the intriguing light b' case, FCNC decays are typically in the $10^{-4} - 10^{-2}$ range, and are quite detectable at the LHC. For a possible future International Linear Collider, we find the associated production of FCNC $e^+e^- \rightarrow b\bar{s}$, $t\bar{c}$ are below sensitivity, while $e^+e^- \rightarrow b'\bar{b}$ and $t'\bar{t}$ can be better probed. Tevatron Run-II can still probe the lighter b' or t' scenario. LHC would either discover the fourth generation and measure the FCNC rates, or rule out the fourth generation conclusively. If discovered, the ILC can study the b' or t' decay modes in detail.

1 Introduction

The successful Standard Model (SM) of electroweak interactions is a renormalizable theory, but it still could be just an effective theory of a more fundamental or more complete theory that is yet to be discovered. The goal of the next generation of high energy colliders, such as the Large Hadron Collider (LHC) [1], or the International Linear Collider (ILC) [2], is to probe the origins of electroweak symmetry breaking, and/or discover new physics phenomena.

The apparent suppression of flavor changing neutral currents (FCNC) has played a critical role in the establishment of the three generation SM. With just one Higgs doublet, by unitarity of the quark mixing matrix, the couplings of neutral bosons (such as the Z boson, Higgs boson, gluon and photon) to a pair of quarks are flavor diagonal at the tree level. At the one loop level, the charged currents (CC) do generate FCNC $Q \rightarrow q\{Z, H, g, \gamma\}$ transitions, but they are suppressed by the GIM mechanism. Interesting phenomena such as CP violation that are the current focus at the B factories involve FCNC $b \rightarrow s$ transitions. Because of very strong GIM cancellation between d , s and b quark loops, and in part because of an unsuppressed decay width, however, the corresponding top decays are rather suppressed [3, 4] in the three generation SM, viz.

$$\mathcal{B}(t \rightarrow cZ) = 1.3 \times 10^{-13}, \quad \mathcal{B}(t \rightarrow cH) = (5.6 - 3.2) \times 10^{-14}, \quad (1)$$

$$\mathcal{B}(t \rightarrow cg) = 3.8 \times 10^{-11}, \quad \mathcal{B}(t \rightarrow c\gamma) = 4.3 \times 10^{-13}, \quad (2)$$

where $M_H = (115 - 130)$ GeV has been taken. Together with the expectation $\mathcal{B}(Z \rightarrow b\bar{s} + \bar{b}s) \cong 10^{-8}$, such strong suppression within three generation SM implies that these processes are excellent probes for new physics, such as supersymmetry, extended Higgs sector, or extra fermion families.

In the last decade, there has been intense activities to explore FCNC involving the top quark. Experimentally, CDF, D0 [5] and LEP II [6] collaborations have reported interesting bounds on FCNC top decays. These bounds are rather weak, however, but will improve in the coming years, first with Tevatron Run II, in a few years with the LHC, and eventually at the ILC. The expected sensitivity to top FCNC at Tevatron Run II is about $\mathcal{B}(t \rightarrow c\gamma) \gtrsim 5 \times 10^{-3}$, while at the LHC, with one year of running, it is possible to probe the range [1, 7],

$$\begin{aligned} \mathcal{B}(t \rightarrow cZ) &\gtrsim 7.1 \times 10^{-5}, & \mathcal{B}(t \rightarrow cH) &\gtrsim 4.5 \times 10^{-5}, \\ \mathcal{B}(t \rightarrow cg) &\gtrsim 10^{-5}, & \mathcal{B}(t \rightarrow c\gamma) &\gtrsim 3.7 \times 10^{-6}. \end{aligned} \quad (3)$$

At the ILC, the sensitivity is slightly less [7], and the range

$$\mathcal{B}(t \rightarrow cH) \gtrsim 4.5 \times 10^{-5}, \quad \mathcal{B}(t \rightarrow c\gamma) \gtrsim 7.7 \times 10^{-6}, \quad (4)$$

can be probed. Thus, models which can enhance these FCNC rates and bring them close to the above sensitivities are welcome.

From the theoretical side, many SM extensions predict that top and Z FCNC rates can be orders of magnitude larger than their SM values (see Ref. [8] for a review). The aim of

this paper is to study FCNC involving heavy quarks in the more modest extension of SM by adding a sequential fourth generation. This retains all the features of SM, except bringing into existence the heavy quarks b' and t' . We will first cover the impact on FCNC top decays: $t \rightarrow cZ, cH, cg, c\gamma$. We find that a 4th generation still cannot bring these decay rates to within experimental sensitivity, once constraints from rare B decays are imposed. Likewise, as discussed in a later section, FCNC decays of the Z boson, e.g. $Z \rightarrow \bar{b}s + \bar{s}b$, also remain difficult.

With LHC in view, however, it is timely to address the decay and detection of 4th generation quarks b' and t' themselves. For this matter, we include in our analysis both CC decays as well as FCNC $b' \rightarrow bX$ and $t' \rightarrow tX$ decays, and evaluate the total widths and branching ratios. We illustrate the search strategies at the LHC (and Tevatron Run-II), and find that FCNC decays are typically at the 10^{-4} – 10^{-2} order, and should be detectable at the LHC. For a relatively light b' just above 200 GeV, FCNC b' decays could still dominate! For completeness, we also study the signature of these FCNC couplings at e^+e^- colliders through heavy and light quark associated production, i.e. FCNC $e^+e^- \rightarrow \bar{b}s + \bar{s}b, \bar{t}c + \bar{c}t, \bar{b}'b + \bar{b}b'$ and $\bar{t}'t + \bar{t}t'$.

Before we turn to our detailed study, we should address the issue as to whether a 4th generation itself is relevant at all. Let us first start with the original motivation for considering a 4th generation. Despite its great success, the 3 generation Standard Model (SM3) may be incomplete. The generation structure (including the question of “Why 3?”) is simply not understood, while having just one heavy quark, the top, with mass at the weak scale is also puzzling. A simple enlargement of SM3 by adding a sequential fourth generation (SM4), where we have already used the notation of t', b' for the fourth generation quarks, could allow us to gain further insight into the question of flavor.

The question that immediately arises is neutrino counting via the invisible Z width [9]. Indeed, one of the original strong motivations for the 4th generation, before the advent of the N_ν result from SLD and LEP experiments, was the possibility of the 4th neutral lepton as a dark matter (DM) candidate. But with active neutrino number N_ν convincingly established at 3, since 1989 the 4th generation as a whole fell out of favor. Recent observations of neutrino oscillations, however, point toward an enlarged neutrino sector [10, 11, 12], which by itself must be beyond minimal SM3. For example, it has been demonstrated recently [13] that, if the right-handed neutrino Majorana mass scale is of the order \mathcal{O} (eV), dubbed “eV seesaw”, a fit to LSND data [14] can be obtained. Within such eV seesaw scenario, unlike the very high scale standard seesaw, extension to the fourth generation can be easily accomplished. In a recent work [11], it has been shown that such eV seesaw can be extended to four lepton generations. The 4th “neutrino” or neutral lepton N is pseudo-Dirac and heavy, so it does not affect the invisible Z width. The 3 extra sterile neutrinos allow one to accommodate LSND data. Taking this as a plausible scenario that $N_\nu = 3$ is no longer an impediment to having a 4th generation, we will not discuss the lepton sector any further in this work.

The second, rather serious issue to face is about precision electroweak constraints, which seem to pose a challenge to the fourth generation. In particular, “an extra generation of ordinary fermions is excluded at the 99.95% CL on the basis of the S parameter

alone” [9], and efforts to reduce S tend to increase T . With $S = -0.04(-0.09) \pm 0.11$, $T = -0.03(+0.09) \pm 0.13$ for $m_H = 100(300)$ GeV, the problem is serious for many extensions beyond SM3, such as technicolor, or SM4 [15]. Even so, for SM4, if the extra neutrino is close to its direct mass limit of $m_N \gtrsim M_Z/2$, this can drive S smaller at the expense of a larger T , and a more detailed analysis suggest a 4th generation is not ruled out [18].

If a 4th generation exists, it will appear soon. The effort of this paper is to update b' and t' decays, including the often dominant charged current decay, to facilitate the search program at Tevatron and LHC. The LHC would either discover the fourth generation and measure some the FCNC rates, or rule out the fourth generation conclusively. In this vein, we mention that there are possible hints for the 4th generation from FCNC and CP violating (CPV) $b \rightarrow s$ transitions at the B factories. The difference in measured [19] direct CPV in $B \rightarrow K^+\pi^-$ and $K^+\pi^0$ modes could arise from New Physics phase in the electroweak penguin process, and the 4th generation is an excellent candidate [20]. Furthermore, the well-known hint [21] of a difference between mixing dependent CPV measurements in a host of charmless $b \rightarrow s\bar{q}q$ type of modes vs $B \rightarrow J/\psi K_S$, dubbed the ΔS problem, could also be partially explained by 4th generation CPV effect through electroweak penguin amplitude [22]. We conclude that the fourth generation is not ruled out, may be hinted at in FCNC/CPV $b \rightarrow s$ transition data, and b' and t' search at the Tevatron and especially the LHC is imperative.

The paper is organized as follows. In the next section we review the experimental constraints from electroweak precision tests, $Z \rightarrow \bar{b}b$, and from FCNC $b \rightarrow s$, $s \rightarrow d$ and $c \rightarrow u$ transitions. In Section 3 we study FCNC $t \rightarrow cX$ decays, and in Section 4 $b' \rightarrow bX$, $t' \rightarrow tX$ decays, where $X = Z, H, g$ and γ . In Section 5 we investigate the associated production $e^+e^- \rightarrow \bar{q}Q + \bar{Q}q$, for $(Q, q) = (b, s), (t, c), (b', b)$ and (t', t) at (Super)B Factories, possible GigaZ, and the future ILC collider. After some discussions in Section 6, our conclusions are given in Section 7. An Appendix deals briefly with suppressed FCNC $b' \rightarrow sX$ and $t' \rightarrow cX$ decays.

2 Constraints

With additional quark mixing elements, one crucial aspect is that the source for CP violation (CPV) is no longer unique. Consideration of CPV phases is important, as it enlarges the allowed parameter space from low energy considerations [23]. Existing experimental data as well as theoretical arguments put stringent constraints on the masses and mixings involving the fourth generation, some of which will be reviewed here.

2.1 CKM Unitarity

Adding a fourth family enlarges the CKM quark mixing matrix, and the present constraint on the various CKM elements V_{ij} for SM3 (i.e. $i, j = 1-3$) that are known only indirectly, are considerably relaxed [9]. Put in other words, flavor physics data do not preclude a 4th generation. For example, the elements $|V_{ts}|$ and $|V_{td}|$ can be as large as about 0.11 and

0.08, respectively [9]. Constraints on CKM elements involving the 4th generation is rather weak. For example, unitarity of the first row of V allows $|V_{ub'}| < 0.08$ [9, 24]. In fact, the long standing puzzle of (some deficit in) unitarity of the first row could be taken as a hint for finite $|V_{ub'}|$.

2.2 Direct Search

Experimental search for fourth generation quarks has been conducted by several experiments. These experimental searches clearly depend strongly on the decay pattern of the fourth generation. A strict bound on b' mass comes from LEP experiments, $m_{b'} \gtrsim M_Z/2$ GeV [25], where both CC and FCNC decays of b' has been considered.

At the Tevatron, where the heavy top quark was discovered, both CDF and D0 have searched for fourth generation quarks. The top quark search applies to b' and t' quarks that decay predominantly into W (i.e. $b' \rightarrow cW$ and $t' \rightarrow bW$), and the corresponding lower bounds are $m_{t',b'} \gtrsim 128$ GeV [26]. Searching for b' quark through its FCNC decays, an analysis by D0 excludes the b' in the mass range $M_Z/2 < m_{b'} < M_Z + m_b$ that decays via the FCNC $b' \rightarrow b\gamma$ process [27]. CDF excludes [28] the b' quark in the mass range of $100 \text{ GeV} < m_{b'} < 199 \text{ GeV}$ at 95% C.L., if $\mathcal{B}(b' \rightarrow bZ) = 100\%$. Assuming $\mathcal{B}(b' \rightarrow bZ) = 100\%$, CDF also excluded long-lived b' quark with mass in the range $M_Z + m_b < m_{b'} < 148 \text{ GeV}$ and a lifetime of $3.3 \times 10^{-11} \text{ s}$ [29]. Recently, CDF has looked for long-lived fourth generation quarks in a data sample of 90 pb^{-1} in $\sqrt{s} = 1.8 \text{ TeV}$ $p\bar{p}$ collisions, by using signatures of muon-like penetration and anomalously high ionization energy loss. The corresponding lower bounds are $m_{t'} \gtrsim 220$ and $m_{b'} \gtrsim 190 \text{ GeV}$ [30].

The above limits can be relaxed if we consider the possibility that $b' \rightarrow bH$, $b' \rightarrow cW$ and $b' \rightarrow bZ$ decays can be of comparable size under certain conditions of the CKM elements [31, 32]. Unless associated CKM elements are extremely small, in general the b' (and certainly the t') quark should not be very long-lived.

2.3 Electroweak and $Z \rightarrow b\bar{b}$ Constraints

Theoretical considerations of unitarity and vacuum stability can put limits on the masses of the fourth generation quarks [10, 33]. Assuming that the fourth family is close to degenerate, perturbativity requires $m_{t',b'} \lesssim 550 \text{ GeV}$.

Even so, for b' and t' below several hundred GeV that we consider, the ρ parameter provides a significant constraint on the splitting between t' and b' , $|m_{t'} - m_{b'}| \lesssim M_W$ [10, 9, 31]. We note that, having the extra neutral lepton close to the current bound of $M_Z/2$ could be accommodated by electroweak data [18], which has now moved [16] much more favorably towards a 4th generation, as discussed in the Introduction.

The Z width is now well measured and provides a good constraint. In particular, t' can contribute to $Z \rightarrow b\bar{b}$ at one loop level. For fixed $m_{t'}$ mass, $V_{t'b}$ can be constrained. Following Ref. [34, 20, 35], for $m_{t'} = 300 \text{ GeV}$ we have,

$$|V_{tb}|^2 + 3.4|V_{t'b}|^2 \leq 1.14, \quad (5)$$

which leads to the bound $|V_{t'b}| \lesssim 0.2$ if we assume that $V_{tb} \approx 1$. The bound is nontrivial, reducing the range for FCNC $b' \rightarrow b$ and $t' \rightarrow t$ rates. But the bound can be relaxed if t' is close to the top quark in mass. In such case, we may still expect large mixing between the third and fourth generation $\sin \theta_{34} \approx \mathcal{O}(1)$.

2.4 $B \rightarrow X_s \gamma$

Let us now consider the constraints from $b \rightarrow s$ transitions such as $B \rightarrow X_s \gamma$ [36] and $B \rightarrow X_s l^+ l^-$ [37]. To study these transitions, we will not use any particular parameterization of the CKM matrix. We will instead argue how large could be the CKM matrix elements that contribute to $b \rightarrow s$ transitions. The unitarity of the 4×4 CKM matrix leads to $\lambda_u + \lambda_c + \lambda_t + \lambda_{t'} = 0$, where $\lambda_f = V_{fs}^* V_{fb}$. In Ref. [23], the effect of a sequential fourth generation on $b \rightarrow s$ transitions has been studied taking into account the presence of a new CP phase in $\lambda_{t'}$. Since $\lambda_u = V_{us}^* V_{ub}$ is very small in strength compared to the others, while $\lambda_c = V_{cs}^* V_{cb} \approx 0.04$, we parameterize $\lambda_{t'} \equiv r_{sb} e^{i\phi_{sb}}$ [20], where ϕ_{sb} is a new CP phase. Then

$$\lambda_t \cong -0.04 - r_{sb} e^{i\phi_{sb}}. \quad (6)$$

With more than three generations and at 90% C.L. [9], the range for $\lambda_t = V_{ts}^* V_{tb}$ is from 0 to 0.12. Such constraint together with Eq. (6) give a bound on r_{sb} which is $r_{sb} \lesssim 0.08$ for all CPV phase $\phi_{sb} \in [0, 2\pi]$. As we shall soon see, such large value for r_{sb} may be in conflict with $\mathcal{B}(B \rightarrow X_s l^+ l^-)$.

Using Eq. (6) and taking into account the GIM mechanism, the amplitude for $b \rightarrow s$ transitions such as $b \rightarrow s \gamma$ and $Z \rightarrow s \bar{b}$ can be written as,

$$\mathcal{M}_{b \rightarrow s} \propto 0.04[f(m_c) - f(m_t)] + r_{sb} e^{i\phi_{sb}} [f(m_{t'}) - f(m_t)], \quad (7)$$

where f is a shorthand for a complicated combination of loop integrals. The relative sign represents the GIM cancellation between top and charm, and t' and top. The usual top effect is located in the first term on the r.h.s. of Eq. (7), while the genuine t' effect is contained in the second term. It is clear that if $\phi_{sb} = 0$, $B \rightarrow X_s \gamma$ will be saturated more quickly. However, for nonvanishing and large CPV phase ϕ_{sb} , the t and t' effects could add in quadrature and the bound becomes more accommodating. Furthermore, the heavy quark mass dependence in the loop integral $f(m_Q)$, $Q = t, t'$, is mild, so GIM cancellation in $f(m_{t'}) - f(m_t)$ is rather strong, hence again accommodating.

The present world average for inclusive $b \rightarrow s \gamma$ rate is [9] $\mathcal{B}(B \rightarrow X_s \gamma) = (3.3 \pm 0.4) \times 10^{-4}$. Keeping the $B \rightarrow X_s \gamma$ branching ratio in the 2σ range of $(2.5-4.1) \times 10^{-4}$ in the presence of the fourth generation, with $m_{t'} = 300$ GeV (400 GeV), we have checked that the allowed range for r_{sb} for all CPV phase ϕ_{sb} is $r_{sb} \in [0, 0.09]$ ($[0, 0.06]$). The allowed range for r_{sb} reduces to 0.03 (0.02) if we allow only 1σ deviation for $b \rightarrow s \gamma$. But for $\phi \sim \pi/2, 3\pi/2$, when $V_{t's}^* V_{t'b}$ is largely imaginary, r_{sb} can take on much larger values [23]. Thus, the $B \rightarrow X_s \gamma$ constraint is not much more stringent than the general CKM constraint.

2.5 $B \rightarrow X_s l^+ l^-$

The inclusive semileptonic $B \rightarrow X_s l^+ l^-$ decay [23] has been measured recently by both Belle and BaBar [38, 39], with rates at $(6.1_{-1.8}^{+2.0}) \times 10^{-6}$ and $(5.6 \pm 1.5 \pm 0.6 \pm 1.1) \times 10^{-6}$ respectively. Both Belle and BaBar have used cuts on the dilepton mass to reduce J/ψ and ψ' charmonium background. For the muon mode, the cuts are $-0.25 \text{ GeV} < M_{\mu\mu} - M_{J/\psi} < 0.10 \text{ GeV}$ and $-0.15 \text{ GeV} < M_{\mu\mu} - M_{\psi(2S)} < 0.10 \text{ GeV}$. For the electron mode, the cut is $m_{e^+e^-} > 0.2 \text{ GeV}$.

With these cuts, for $m_{t'} = 300$ (400) GeV and allowing $B \rightarrow X_s l^+ l^-$ to be within the 2σ range of the experimental value of $(6.1_{-1.8}^{+2.0}) \times 10^{-6}$, we find that $r_{sb} \lesssim 0.02$ (0.01) for all CPV phase ϕ_{sb} . The more stringent bounds apply, however, for $\phi_{sb} \approx \pi$ when t' and t effects are constructive. They can be considerably relaxed for CPV phase $\phi_{sb} \lesssim \pi/2$ and $\phi_{sb} \gtrsim 3\pi/2$. For $m_{t'} = 300 \text{ GeV}$ and $\phi_{sb} = 0$, $r_{sb} = 0.07$ can still be tolerated. We see that the bounds on r_{sb} from $B \rightarrow X_s l^+ l^-$ are more restrictive than those coming from $B \rightarrow X_s \gamma$.

Our bounds on r_{sb} are similar to the finding of Refs. [34, 20]. Note that Ref. [34] does not use $b \rightarrow s \gamma$ constraint and consider many others, and the bound on r_{sb} seems to come from $b \rightarrow X_s l^+ l^-$. We stress in closing that $B_s - \bar{B}_s$ can constrain only slightly $r_{sb} e^{i\phi_{sb}}$ [23], but rules out some region around $\phi_{sb} \sim 0$ and large r_{sb} [20], when there is too much destruction between t' and t effect.

2.6 $c \rightarrow u, s \rightarrow d$ and $b \rightarrow d$ transitions

As seen in the previous sections, $B \rightarrow X_s \gamma$, $B \rightarrow X_s l^+ l^-$ and $B_s^0 - \bar{B}_s^0$ mixing can constrain $\lambda_{t'} = r_{sb} e^{i\phi_{sb}}$ for given $m_{t'}$. This would have implications on $Z \rightarrow \bar{s}b + s\bar{b}$, as well as $t \rightarrow c$ transitions. To further constrain the 4×4 CKM matrix elements, one can consider other observables such as $D^0 - \bar{D}^0$ mixing and rare kaon decays $K_L \rightarrow \mu^+ \mu^-$, $K^+ \rightarrow \pi^+ \nu \bar{\nu}$, ϵ'/ϵ , and $B_d - \bar{B}_d$ mixing and associated CP violation.

Recent search for $D^0 - \bar{D}^0$ mixing [9] puts an upper bound on the mixing amplitude $|M_{12}^D| \leq 6.2 \times 10^{-14} \text{ GeV}$ at 95% C.L. [40]. In this bound CP violation in the mixing has been included. Assuming that the long distance contributions to the mixing amplitude are small, one can constrain the fourth generation parameters, namely $m_{t'}$ and $|V_{ub'}^* V_{cb'}|$. For fixed $m_{t'}$, and using analytic formula from [34, 41], we get a bound on $|V_{ub'}^* V_{cb'}|$ as

$$|V_{ub'}^* V_{cb'}| \lesssim \begin{cases} 7 \times 10^{-3}, & m_{t'} = 240 \text{ GeV}, \\ 5.1 \times 10^{-3}, & m_{t'} = 360 \text{ GeV}. \end{cases} \quad (8)$$

The bound can be easily satisfied with a small $V_{ub'}$, which we would in general assume.

It has been demonstrated in [34, 20] that $V_{t'd}^* V_{t's}$ is well constrained by $\mathcal{B}(K^+ \rightarrow \pi^+ \nu \bar{\nu})$, $K_L \rightarrow \mu^+ \mu^-$ and ϵ_K . From Ref. [20] and for $m_{t'} = 300 \text{ GeV}$, one can read that $|V_{t'd}^* V_{t'd}|$ up to 7×10^{-4} is tolerated both by ϵ_K as well as by $\mathcal{B}(K^+ \rightarrow \pi^+ \nu \bar{\nu})$, even for sizable $r_{sb} \sim 0.025$.

Overall, however, we will not be concerned with FCNC constraints involving the first generation, except for discussions on $Z \rightarrow \bar{s}b + s\bar{b}$ and $t \rightarrow c$ transitions. For FCNC

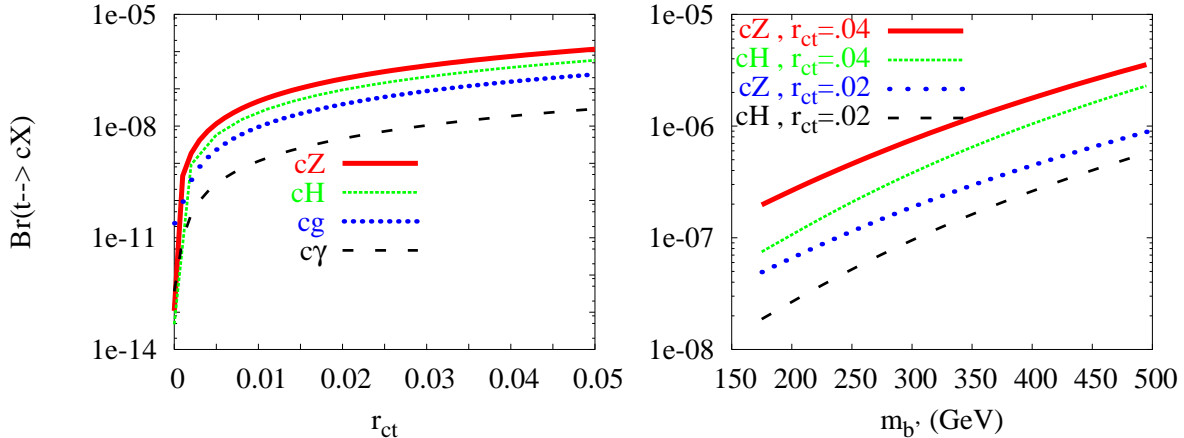


Figure 1: Fourth generation effect on $t \rightarrow c\{Z, H, g, \gamma\}$ rate, with $M_H = 115$ GeV, $m_{b'} = 300$ GeV (left) and $r_{ct} = 0.02, 0.04$ (right).

transitions involving b' and t' , we will simply decouple the first generation and not be concerned with the associated constraints discussed here. The second generation, however, is important, as we shall see.

3 FCNC $t \rightarrow cX$ Decays

We now investigate FCNC involving heavy quarks with four generation effect, which is the main focus of this paper. We start with $t \rightarrow cZ, cH, cg, c\gamma$ decays in this section, turning to $b' \rightarrow bZ, bH, bg, b\gamma$ as well as $t' \rightarrow tZ, tH, tg, t\gamma$ in the next section.

To the best of our knowledge, the contribution from a sequential fourth generation to top FCNC $t \rightarrow cZ, cH, cg$ and $c\gamma$ has not yet been discussed. The unitarity of the 4×4 CKM matrix is expressed as

$$\lambda_d + \lambda_s + \lambda_b + \lambda_{b'} = 0, \quad (9)$$

where $\lambda_f = V_{cf}V_{t'f}^*$. In our analysis we shall parameterize $\lambda_{b'} = V_{cb'}V_{t'b'}^* \equiv r_{ct}e^{i\phi_{ct}}$. Although naively the allowed range for r_{ct} by unitarity is rather large, however, the strength of r_{ct} is correlated with the strength of r_{sb} by unitarity. In the standard parameterization of 4×4 CKM [42], Ref. [20] has shown that for $m_{t'} = 300$ GeV, one finds $|r_{ct}| = |\lambda_{b'}| = |V_{cb'}V_{t'b'}^*| \lesssim 0.025$. As we shall see below, for $t \rightarrow c$ transitions, $\lambda_d, \lambda_s, \lambda_b$ turn out to be numerically irrelevant, and only $\lambda_d + \lambda_s + \lambda_b = -\lambda_{b'}$ matters. In what follows, to give an idea on the size of the fourth generation effect on FCNC decays involving the top quark, we will relax the $|r_{ct}| \lesssim 0.025$ bound and take it to be in the range of 0 to 0.05.

To discuss the numerical effects on all $t \rightarrow c$ transitions, we fix our parameters as follows: $(m_t, m_b, m_c, m_s) = (174.3, 4.7, 1.5, 0.2)$ GeV, $\alpha^{-1} \approx 128$, $\alpha_s(m_t) \approx 0.105$. The top width is taken as $\Gamma_t = 1.55$ GeV. All the computations of FCNC decay rates are done with the help of the packages FeynArts, FormCalc [43], and with LoopTools and FF for numerical evaluations [44, 45]. The one-loop amplitudes are evaluated in the 't

Hooft–Feynman gauge using dimensional regularization. Cross checks with well known SM FCNC processes are made, and perfect agreement has been found. The numbers we show in Eqs. (1) and (2) for example, were obtained by FormCalc [43].

We have checked that the results for $t \rightarrow cX$ do not depend on light quark masses m_d , m_s , m_c and m_b for any finite r_{ct} , hence the one loop amplitudes $\mathcal{M}_{t \rightarrow c}$ can be approximated as,

$$\mathcal{M}_{t \rightarrow c} \propto r_{ct} e^{i\phi_{ct}} [f(m_{b'}) - f(0)], \quad (10)$$

where f is some loop integral with implicit external quark mass dependence, and light internal quark effects are summarized in $f(0)$. It is clear from Eq. (10) that the CPV phase ϕ_{ct} will not affect $t \rightarrow c$ transition rates at all.

In Fig. 1 we illustrate $\mathcal{B}(t \rightarrow \{cZ, cH, cg, c\gamma\})$ vs r_{ct} for $m_{b'} = 300$ GeV (left plot), and vs $m_{b'}$ (right plot) for $r_{ct} = 0.02$ and 0.04 . $M_H = 115$ GeV is assumed. The branching ratios are not sensitive to the CPV phase ϕ_{ct} which has been dropped. As can be seen from the left plot, we reproduce the SM results for $\mathcal{B}(t \rightarrow \{cZ, cH, cg, c\gamma\})$ when $r_{ct} = 0$ (where the lighter quark masses are kept). As r_{ct} increases, all branching ratios can increase by orders of magnitude. For large $r_{ct} = 0.04$ and rather heavy $m_{b'} \gtrsim 350$ GeV, branching ratios for $t \rightarrow cZ$ and $t \rightarrow cH$ can reach $\approx 10^{-6}$. But such large values of r_{ct} and $m_{b'}$, combined, may run into difficulty with $b \rightarrow s$ transitions.

We see that $t \rightarrow cZ$ is much more enhanced compared to $t \rightarrow cg$ and $t \rightarrow c\gamma$. This is due to the fact that the axial coupling of the Z boson is related to the unphysical Goldstone boson, which is the partner of the physical Higgs boson before symmetry breaking. Thus, the non-conserved part of the Z coupling has a rather similar dependence on heavy internal quark masses as the Higgs coupling, and both show nondecoupling of SM heavy quarks in loop effects. For $t \rightarrow cg$ and $t \rightarrow c\gamma$, they do not have this behavior because gauge invariance demands conserved currents, and the heavy quark effects in the loop are basically decoupled.

We conclude that fourth generation contributions can enhance top FCNC couplings by orders of magnitude with respect to SM values, reaching 10^{-7} – 10^{-6} for $t \rightarrow cZ, cH$. But such enhanced rates seem to be still out of experimental reach for the foreseeable future. Nevertheless, search for FCNC $t \rightarrow c$ decays should continue.

4 FCNC $b' \rightarrow bX$ and $t' \rightarrow tX$ transitions

As mentioned above, EW precision measurements constrain $|m_{t'} - m_{b'}| \lesssim M_W$. This constraint does not imply that t' is heavier than b' . Therefore, we shall address b' and t' decays for both $m_{b'} < m_{t'}$ and $m_{b'} > m_{t'}$ situations.

Before describing our strategy for FCNC $b' \rightarrow b$ and $t' \rightarrow t$ decays, we review first the tree level decays of b' and t' . The possible Charged Current tree level decay modes are,

$$\begin{aligned} b' &\rightarrow cW, tW^{(*)}, t'W^*; \\ t' &\rightarrow sW, bW, b'W^*. \end{aligned} \quad (11)$$

Due to expected suppression of the CKM elements $V_{ub'}$ and $V_{t'd}$, the CC $b' \rightarrow uW$ and $t' \rightarrow dW$ decays will be neglected in what follows. Since EW measurements constrain the splitting between t' and b' to be less than about the W mass, the decay $t' \rightarrow b'W^*$ or $b' \rightarrow t'W^*$ can occur only with a virtual W^* decaying as $W^* \rightarrow f_1f_2$. For the tree decays $t', b' \rightarrow \{b'; t, t'\}W^* \rightarrow \{b'; t, t'\}f_1f_2$ involving off-shell W and heavy quark final state, we have used the analytic expression from [46] and included all the light fermion channels by using $\Gamma(Q' \rightarrow QW^*) = 9\Gamma(Q' \rightarrow Qe\nu_e)$. In the following discussion of FCNC decays, we will refrain from discussing the three body decays $b' \rightarrow bf\bar{f}$ and $t' \rightarrow tf\bar{f}$, with f any light fermions or neutrinos. These decays could be comparable to $b' \rightarrow b\gamma$ or $t' \rightarrow t\gamma$ [47].

Turning to FCNC $b' \rightarrow b$ and $t' \rightarrow t$ transitions, we note that FCNC b' decays have been extensively studied in the literature [31, 46, 47, 48, 49, 50]. Here, we update those studies and investigate t' decays also, taking into account recent experimental measurements. Motivated by the above constraints on CKM matrix elements, in studying loop induced $b' \rightarrow b$ and $t' \rightarrow t$ transitions, we will decouple the first and second generations quarks. Therefore, the relevant CKM matrix will be effectively 2×2 and *real*. The one-loop amplitudes take the following forms:

$$\mathcal{M}_{b' \rightarrow b} \propto r_{bb'}[f(m_{t'}) - f(m_t)], \quad (12)$$

$$\mathcal{M}_{t' \rightarrow t} \propto r_{tt'}[f(m_{b'}) - f(0)], \quad (13)$$

where $r_{bb'} = V_{t'b}^*V_{t'b'}$, $r_{tt'} = V_{tb'}V_{t't}^*$. Note that the near degeneracy of light m_d , m_s and m_b at the t, b', t' scale makes Eq. (13) a good approximation without the assumption of neglecting the first two generations. Since $V_{t'b'} \approx \mathcal{O}(1)$, $|r_{bb'}|$ and $|r_{tt'}|$ are almost the same. From the discussion in Section 2, we will take $r_{bb'}$ in the range $0.05 - 0.25$. It is clear from Eqs. (12) and (13) that the rates of FCNC $b' \rightarrow b$ and $t' \rightarrow t$ decays will increase with $r_{bb'}$. Like the $t \rightarrow c$ transition, we expect that the mode $b' \rightarrow bZ$ and $b' \rightarrow bH$ will dominate over $b' \rightarrow b\gamma$ and $b' \rightarrow bg$. We have checked numerically that, as long as $|V_{cb'}|, |V_{t's}| \lesssim 0.06$, assuming 2×2 form in the 3rd and 4th generation sector and considering only $b' \rightarrow b$ and $t' \rightarrow t$ transitions is a good approximation. This is because of the lightness of the first 2 generations, as well as the expected smallness of product of CKM elements. In the Appendix, we give a comparison of the rates of suppressed $b' \rightarrow sX$, $t' \rightarrow cX$ decays with respect to $b' \rightarrow bX$, $t' \rightarrow tX$, which will depend on the CKM elements $V_{t's}$ and $V_{cb'}$.

4.1 Internal and External m_Q Dependence

Unlike the $t \rightarrow cX$ case, where there is one internal and one external heavy quark each, with m_t already fixed, $b' \rightarrow bX$ decay involves two internal and one external heavy quarks, while $t' \rightarrow tX$ decay involves one internal and two external heavy quarks. Before presenting our results for total width and branching ratios, it is useful to discuss the sensitivity of the FCNC $b' \rightarrow b$ and $t' \rightarrow t$ decay widths to both internal and external heavy quark masses. To this end we give in Figs. 2 and 3 the decay widths $\Gamma(b' \rightarrow bX)/r_{bb'}^2$ and $\Gamma(t' \rightarrow tX)/r_{tt'}^2$ for $X = Z, H, g, \gamma$. For a fixed $m_{b'}$ (or fixed $m_{t'}$) value, by the $\delta\rho$ constraint, the allowed range for $m_{t'}$ (or $m_{b'}$) should be within $|m_{b'} - m_{t'}| \lesssim M_W$. But for sake of illustration, we will plot outside of such constraint.

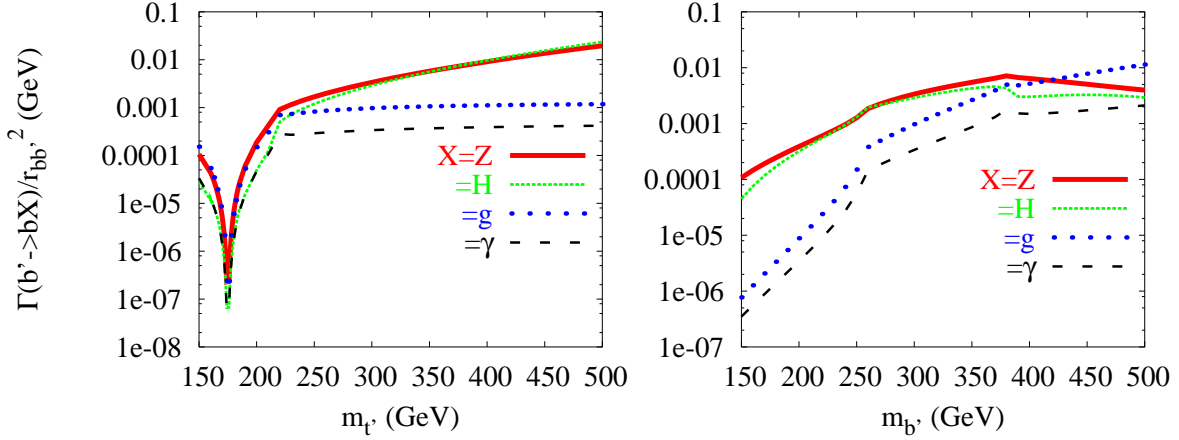


Figure 2: Decay width of $\Gamma(b' \rightarrow b\{Z, H, g, \gamma\})$ normalized to $r_{bb'}^2$ as a function of $m_{t'}$ for $m_{b'} = 300$ GeV (left), and as function of $m_{b'}$ for $m_{t'} = 300$ GeV (right).

In Fig. 2(a), we show $\Gamma(b' \rightarrow bX)/r_{bb'}^2$ as function of $m_{t'}$ in the 150–500 GeV range, with $m_{b'}$ held fixed at 300 GeV. The big dip at $m_{t'} \sim m_t$ illustrates the GIM cancellation of Eq. (12), while the kink around $m_{t'} \sim 220$ GeV corresponds to $b' \rightarrow t'W$ cut. Above the kink, the $b' \rightarrow bZ$ and bH widths grow with increasing $m_{t'}$ because of the rising t' Yukawa coupling. The $b' \rightarrow bg$ and $b' \rightarrow b\gamma$ modes, however, stay almost constant. This is due to decoupling of the t' quark for large $m_{t'}$, and the effect largely comes from the top. Thus, as one can see from the plot, around $m_{t'} \sim 220$ GeV one has $\Gamma(b' \rightarrow bZ) \gtrsim \Gamma(b' \rightarrow bg) \gtrsim \Gamma(b' \rightarrow bH) > \Gamma(b' \rightarrow b\gamma)$. But for $m_{t'} \sim 500$ GeV, one has $\Gamma(b' \rightarrow bH) \gtrsim \Gamma(b' \rightarrow bZ) > \Gamma(b' \rightarrow bg) > \Gamma(b' \rightarrow b\gamma)$, and $\Gamma(b' \rightarrow b\{Z, H\})/r_{bb'}^2$ are slightly above $0.01/r_{bb'}^2$ GeV.

In Fig. 2(b), we plot $\Gamma(b' \rightarrow bX)/r_{bb'}^2$ as a function of the decaying particle mass $m_{b'}$ for $m_{t'}$ fixed at 300 GeV. Obviously, $\Gamma(b' \rightarrow bX)/r_{bb'}^2$ increase with increasing $m_{b'}$ just from phase space. Above the $b' \rightarrow t'W$ threshold at 255 GeV, the increase in rate with $m_{b'}$ slows, more so for the $b' \rightarrow bZ$ and bH modes. The $b' \rightarrow bg$ mode becomes comparable to $b' \rightarrow bZ$ and bH modes as the $b' \rightarrow t'W$ threshold of 380 GeV is approached. Passing this threshold, interestingly, the $b' \rightarrow bZ$ and bH widths start to decrease slightly with $m_{b'}$, the external mass. The $b' \rightarrow bg, b\gamma$ modes, however, continue to rise with phase space, and $b' \rightarrow bg$ becomes the dominant mode above 400 GeV.

We illustrate $\Gamma(t' \rightarrow tX)/r_{t't'}^2$ in Fig. 3 as a function of $m_{b'}$ (left) and $m_{t'}$ (right). As one can see from Fig. 3(a), it is remarkable that $\Gamma(t' \rightarrow tg)$ is about one order of magnitude larger than $\Gamma(t' \rightarrow t\{Z, H, \gamma\})$ for $m_{b'} < 220$ GeV, when $t' \rightarrow b'W$ is open. Note that the gluon can only be radiated off the $b^{(l)}$ quark, while Z, H and γ can also radiate off the W boson. For $m_{b'} > 220$ GeV, the b' decouples from $t' \rightarrow tg$, and $t\gamma$ and these widths decrease as $m_{b'}$ increase. But $\Gamma(t' \rightarrow t\{Z, H\})$ grow rapidly with increasing $m_{b'}$. One can see also that $t' \rightarrow tH$ width increases more rapidly with $m_{b'}$ as one passes through $b'W$ threshold, and remains considerably larger than $b' \rightarrow bZ$ for large $m_{b'}$.

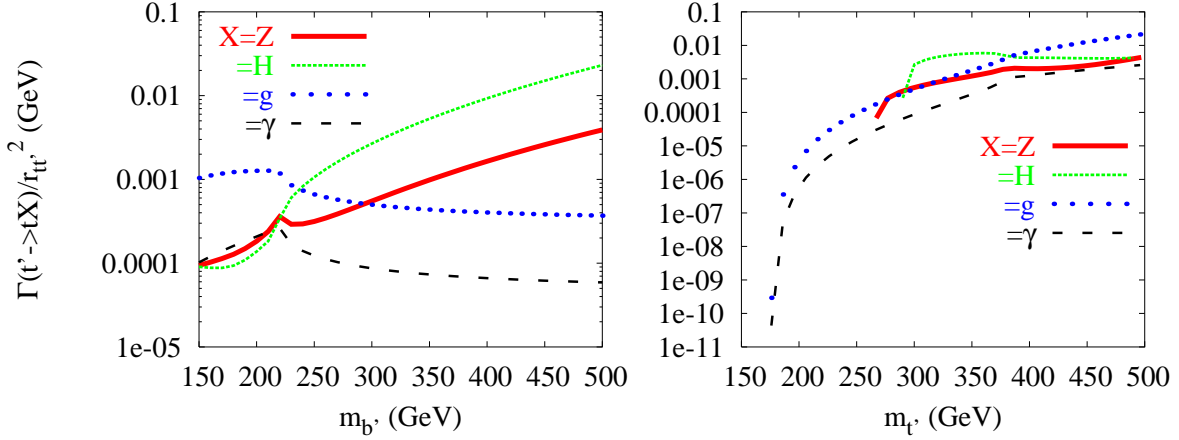


Figure 3: Decay width of $\Gamma(t' \rightarrow t\{Z, H, g, \gamma\})$ normalized to $r_{tt'}^2$ as a function of $m_{b'}$ for $m_{t'} = 300$ GeV (left), and as function of $m_{t'}$ for $m_{b'} = 300$ GeV (right).

In Fig. 3(b), we illustrate $\Gamma(t' \rightarrow tX)/r_{tt'}^2$ as function of $m_{t'}$, for $m_{b'} = 300$ GeV held fixed. Of course both $t' \rightarrow tZ$ and $t' \rightarrow tH$ are open only for $m_{t'} > m_t + m_Z$ and $m_{t'} > m_t + M_H$ respectively. Once the Higgs decay mode is open it dominates over Z and gluon modes. But when $m_{t'}$ crosses 380 GeV, the $t' \rightarrow b'W$ threshold, the gluon mode starts to dominate over the other three decay modes. This behavior is similar to what is seen in Fig. 3(a) for lower b' and t' masses.

The FCNC widths considered in the following subsections are special cases of those presented in Figs. 2 and 3.

4.2 b' and t' Widths

For illustration, we fix $m_{t'} = 300$ GeV and consider the cases of $m_{b'} = 240$ GeV to illustrate $m_{b'} < m_{t'}$, and $m_{b'} = 360$ GeV to illustrate $m_{b'} > m_{t'}$. We shall use the examples of $|V_{cb'}| \approx |V_{t's}| \approx V_{cb} \approx 0.04$ and $|V_{cb'}| \approx |V_{t's}| = 10^{-3}$ to illustrate sizable versus suppressed $V_{cb'}$. The results for intermediate strength $|V_{cb'}| \approx |V_{t's}|$ can be inferred from our plots given in the next two subsections.

Let us first give the estimates of different decay widths that contribute to b' and t' decays. For b' , the FCNC and CC tree level decay widths are given (in GeV) as:

$$\Gamma(b' \rightarrow bZ, bH, bg, b\gamma) = \begin{cases} (0.98, 0.95, 0.07, 0.028) \times 10^{-3} r_{bb'}^2, & m_{b'} = 240 \text{ GeV}, \\ (0.61, 0.45, 0.33, 0.11) \times 10^{-2} r_{bb'}^2, & m_{b'} = 360 \text{ GeV}, \end{cases} \quad (14)$$

$$\Gamma(b' \rightarrow cW, tW^{(*)}, t'W^{(*)}) = \begin{cases} 4.38|V_{cb'}|^2, 0.0046|V_{tb'}|^2, 0, & m_{b'} = 240 \text{ GeV}, \\ 15.2|V_{cb'}|^2, 6.66|V_{tb'}|^2, 0.0031, & m_{b'} = 360 \text{ GeV}, \end{cases} \quad (15)$$

where $V_{t'b'} \simeq 1$ is assumed. The total decay width is then (in GeV)

$$\Gamma_{b'} = \begin{cases} 0.007r_{bb'}^2 + 4.38|V_{cb'}|^2, & m_{b'} = 240 \text{ GeV}, \\ 6.68r_{bb'}^2 + 15.2|V_{cb'}|^2 + 0.0031, & m_{b'} = 360 \text{ GeV}. \end{cases} \quad (16)$$

Note that we shall take $|V_{tb'}|$ for tree and $|V_{tb}^*V_{tb'}| \simeq |V_{t'b'}V_{tb}^*| \simeq |r_{bb'}|$ for loop as the same strength in our plots for simplicity. We have thus combined the $b' \rightarrow tW^{(*)}$ and $b' \rightarrow bX$ widths in Eq. (16).

For t' , one has (in GeV)

$$\Gamma(t' \rightarrow tZ, tH, tg, t\gamma) = \begin{cases} (0.29, 0.83, 0.74, 0.14) \times 10^{-3} r_{tt'}^2, & m_{b'} = 240 \text{ GeV}, \\ (1.1, 6.1, 0.43, 0.07) \times 10^{-3} r_{tt'}^2, & m_{b'} = 360 \text{ GeV}, \end{cases} \quad (17)$$

$$\Gamma(t' \rightarrow bW, sW, b'W^*) = \begin{cases} 8.72|V_{tb'}|^2, 8.73|V_{t's}|^2, 0.003, & m_{b'} = 240 \text{ GeV}, \\ 8.72|V_{t'b}|^2, 8.73|V_{t's}|^2, 0, & m_{b'} = 360 \text{ GeV}, \end{cases} \quad (18)$$

where $V_{t'b'} \simeq 1$ is assumed. The total decay width is (in GeV)

$$\Gamma_{t'} = \begin{cases} 8.72r_{tt'}^2 + 8.73|V_{t's}|^2 + 0.003, & m_{b'} = 240 \text{ GeV}, \\ 8.73r_{tt'}^2 + 8.73|V_{t's}|^2, & m_{b'} = 360 \text{ GeV}. \end{cases} \quad (19)$$

Again we shall take $|V_{t'b}| \simeq |V_{t'b}^*V_{tb}| \simeq |V_{t'b'}^*V_{tb'}| \simeq |r_{tt'}|$ in our plots for simplicity. So $t' \rightarrow bW^{(*)}$ and $t' \rightarrow tX$ widths are combined in Eq. (19).

It is clear from the above equations that in general the CC decays $b' \rightarrow \{cW, tW\}$ and $t' \rightarrow \{bW, sW\}$ would dominate b' and t' rates, respectively. One may think that the $b' \rightarrow cW$ and $t' \rightarrow sW$ decays should be subdominant since $|V_{t's}|^2 \approx |V_{cb'}|^2 \ll |V_{t'b}|^2 \approx |V_{tb'}|^2$ seem plausible. However, in the plausible HNS scenario [20] which we will discuss later, $|V_{t's}|^2 \approx |V_{cb'}|^2$ is not much smaller than $|V_{t'b}|^2 \approx |V_{tb'}|^2$, and the $b' \rightarrow cW$ and $t' \rightarrow sW$ decays can compete with $b' \rightarrow tW$ and $t' \rightarrow bW$, and could even dominate. For the lighter $m_{b'} = 240$ GeV case, if $|V_{cb'}| \ll r_{bb'}$ then $b' \rightarrow cW$ is CKM suppressed, and FCNC $b' \rightarrow bZ, bH$ are comparable to $b' \rightarrow tW^*$. The latter could be further suppressed if $m_{b'} < 240$ GeV. But depending on the level of suppression for $|V_{cb'}|$, $b' \rightarrow cW$ could also be comparable with the loop-induced FCNC $b' \rightarrow bZ$ and $b' \rightarrow bH$ decays. Such a scenario has been studied in Ref. [31] with $m_{b'} \lesssim 200$ GeV and where it has been assumed that $|V_{cb'}/(V_{t'b'}V_{tb}^*)| \approx 10^{-3}$. It is still relevant at the Tevatron.

4.3 Phenomenology of b' Decay

We show in Fig. 4(a) the various b' decay branching ratios for $|V_{cb'}| = 0.04 \sim V_{cb}$. In this case, the $b' \rightarrow cW$ process is the dominant decay mode for $m_{b'} = 240$ GeV, which illustrates $m_{b'} < m_{t'}$. Thus, one should search for $b'\bar{b}'$ via $c\bar{c}W^+W^-$. The loss of b -tagging as a powerful tool will make this study more challenging. The off-shell W decay $b' \rightarrow tW^*$ is open but is in the range of 10^{-3} – 10^{-2} . The size of the loop-induced FCNC $b' \rightarrow bZ, bH$ decays is of order 10^{-3} , but could be larger for a lighter b' . Such strength for FCNC is sizable when compared with $t \rightarrow cX$. According to Eq. (3), top FCNC of the order 10^{-5} can be measured at LHC or ILC. For heavier quarks such as b' and t' , the production cross sections are smaller than $t\bar{t}$ case, resulting in a smaller number of events. We therefore expect that the sensitivity to heavy quark FCNC decays will be less than what we have listed in Eq. (3). Still, it should be promising to probe heavy quark FCNC decays up to the

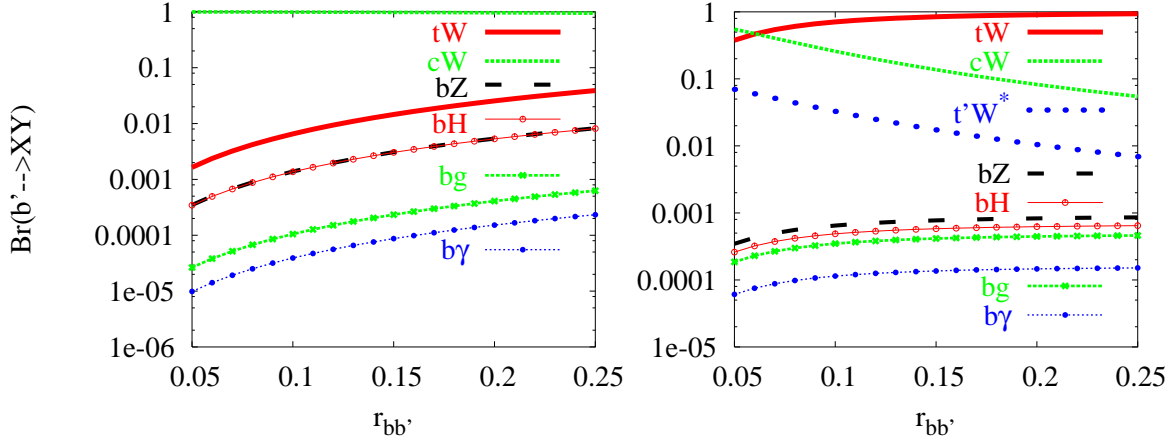


Figure 4: Branching ratios for b' vs $r_{bb'}$ for $m_{b'} = 240$ GeV (left), 360 GeV (right), with $m_{t'} = 300$ GeV and $|V_{cb'}| = 0.04$.

order 10^{-3} at the LHC or ILC. A higher luminosity run and/or a higher energy machine would improve the sensitivity.

The results for $m_{b'} = 360 > m_{t'} = 300$ GeV is given in Fig. 4(b), where the b' decay channels are richer. The $b' \rightarrow t'W^*$ mode is now open but still subdominant. Since $m_{b'}$ is higher, the decay $b' \rightarrow tW$ is enhanced to over 30% for small $r_{bb'} \approx 0.05$, and approaches 100% for large $r_{bb'}$ approaching $\mathcal{O}(\lambda)$. For $r_{bb'} \gtrsim 0.06$ and $|V_{cb'}| = 0.04$, $b' \rightarrow tW$ dominates over $b' \rightarrow cW$ mode. $|V_{cb'}| > 0.04$ would delay the dominance of tW^* over cW , but for $|V_{cb'}| < 0.04$, the $b' \rightarrow cW$ mode will be further suppressed. The search strategy should be via $b'\bar{b}' \rightarrow t\bar{t}W^+W^- \rightarrow b\bar{b}W^+W^-W^+W^-$, which has 4 W bosons. However, depending on strength of $b' \rightarrow cW$, one could have $t\bar{c}W^+W^-$, $c\bar{c}W^+W^-$, resulting in 3 or 2 W bosons only, with reduced b -tagging discrimination. The $t'W^*$ mode would pose a further challenge with off-shell W s. For the FCNC decays, note that $b' \rightarrow bg$ is close to bZ and bH rate of the order 10^{-3} , while $b' \rightarrow b\gamma$ is at 10^{-4} order. The LHC should be able to probe a major part of this range of rates.

For $|V_{cb'}|$ as small as 10^{-3} , as can be seen from Fig. 5(a), for $m_{b'} = 240$ GeV and $m_{t'} = 300$ GeV, $b' \rightarrow tW^*$ is the dominant mode for $r_{bb'}$ in range of 0.05–0.25, with bZ and bH comparable. The study of $b'\bar{b}' \rightarrow t\bar{t}W^*W^*$ should be undertaken. The off-shell nature of the W would make it somewhat more troublesome. Since $b' \rightarrow bZ$, bH could easily be a few 10% (e.g. a slightly lighter b'), one should really be searching for $t\bar{t}W^*W^*$, $t\bar{b}W^*Z$, $t\bar{b}W^*H$, $b\bar{b}Z$, $b\bar{b}H$ simultaneously, which is a rewarding if not complicated program. Furthermore, since $b' \rightarrow tW^*$ is highly sensitive to $m_{b'}$, and could be suppressed by smaller $m_{b'} < 240$ GeV, the FCNC $b' \rightarrow bZ, bH$ decays could still dominate for relatively light $m_{b'}$ just above 200 GeV. This could help uncover the Higgs boson [31]! For $r_{bb'} \approx 0.05$, $b' \rightarrow cW$ is just below $b' \rightarrow bZ$ and bH . Its branching ratio decreases for larger $r_{bb'}$, becoming comparable in size with $b' \rightarrow bg > b\gamma$ at the 10^{-2} level as $r_{bb'}$ approaches 0.2. The $b' \rightarrow b\gamma$ mode is at a few $\times 10^{-3}$. Thus, this scenario of relatively light b' and very

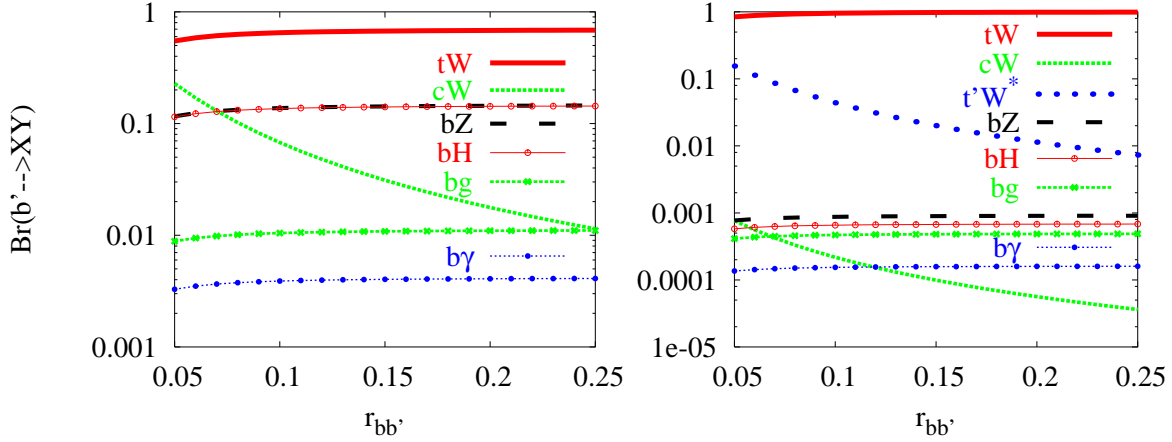


Figure 5: Same as Fig. 4 with $|V_{cb'}| = 10^{-3}$.

suppressed $V_{cb'}$ is the most interesting one for FCNC b' decays.

For $m_{b'} = 360$ GeV and $m_{t'} = 300$ GeV, as seen in Fig. 5(b), $b' \rightarrow tW$ is now fully open and is of order 100% for the full range of $r_{bb'}$. It is followed by $b' \rightarrow t'W^*$ with rates in the range of (1 – 10)%, since $V_{t'b'} \cong 1$, dropping as $r_{bb'}$ increases. In this case of heavy $m_{b'}$, the FCNC $b' \rightarrow bZ$, bH and bg decays are comparable and just below 10^{-3} , with $b' \rightarrow b\gamma$ just below at a few $\times 10^{-4}$ in rate. Compared to $t \rightarrow cX$, even to $b \rightarrow sX$, these are still rather sizable rates for FCNCs, and in view of Eq. (3), they can be probed at the LHC if the heavy quarks are not too heavy. The FCNCs are dominant over CC $b' \rightarrow cW$ decay for $r_{bb'} \gtrsim 0.1$, which is at the 10^{-4} order or less.

There is, therefore, a rather broad range of possibilities for b' decay, depending on $m_{b'}$, $V_{cb'}$ and $V_{t'b'}$. For $m_{b'} \lesssim 240$ GeV and very small $V_{cb'}$, FCNC dominance is possible [31]. For $m_{b'} > m_t + M_W$, the dominance of $b' \rightarrow tW$ implies $b'\bar{b}' \rightarrow t\bar{t}W^+W^- \rightarrow b\bar{b}W^+W^+W^-W^-$, or $4W$ s plus 2 b -jets, which should be of interest at LHC. In between, the signal varies in richness and complexity, but the FCNC are always within reach at the LHC.

4.4 Phenomenology of t' Decay

Let us turn now to t' decays. As shown in Figs. 6 and 7 for $m_{t'} = 300$ GeV, $t' \rightarrow bW$ is fully open and dominates over $t' \rightarrow sW$ for $|V_{t's}| \approx |V_{cb'}| \approx 0.04$.

For $m_{t'} > m_{b'}$, as illustrated by Fig. 6(a) for $m_{b'} = 240$ GeV, the decay mode $t' \rightarrow b'W^*$ is open but kinematically suppressed, and its branching ratio is in the range of 10^{-2} – 10^{-1} . In the case of enhanced $|V_{t's}| \gtrsim 0.04$, $t' \rightarrow sW$ could in principle dominate over $t' \rightarrow bW$ mode. For the FCNC decays, note that $t' \rightarrow tH$ and tg are comparable at 10^{-4} order, with tZ slightly below, followed by $t\gamma$ around 10^{-5} order. Though more difficult than b' case, these rates are above the $t \rightarrow cX$ rates, and may be measurable at the LHC.

For $m_{t'} < m_{b'}$ as illustrated by Fig. 6(b), the $t' \rightarrow b'W^*$ decay is forbidden. With the heavier b' , the $t' \rightarrow tH$ rate is raised to close to 10^{-3} , followed by $t' \rightarrow tZ$, which is slightly

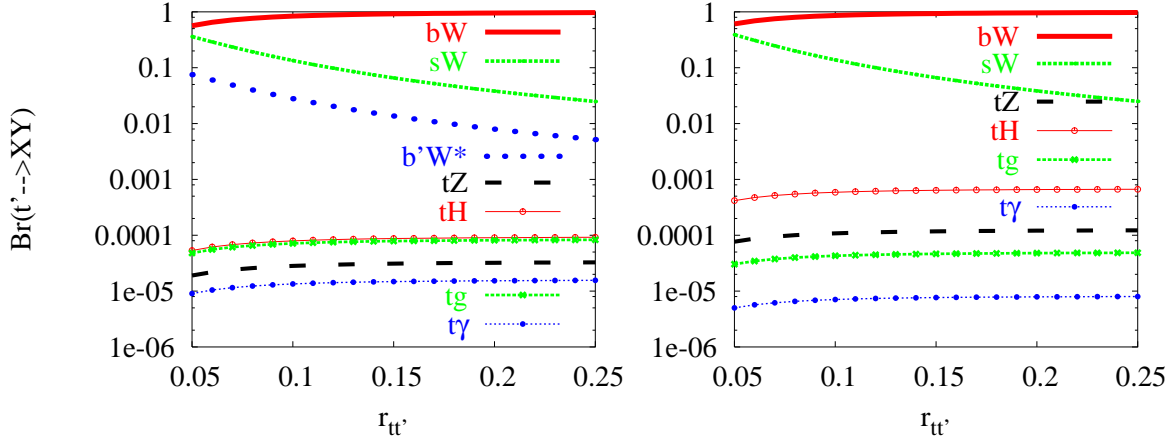


Figure 6: Branching ratio for t' vs $r_{tt'}$ for $m_{b'} = 240$ GeV (left), 360 GeV (right), with $m_{t'} = 300$, and $|V_{cb'}| = |V_{t's}| = 0.04$.

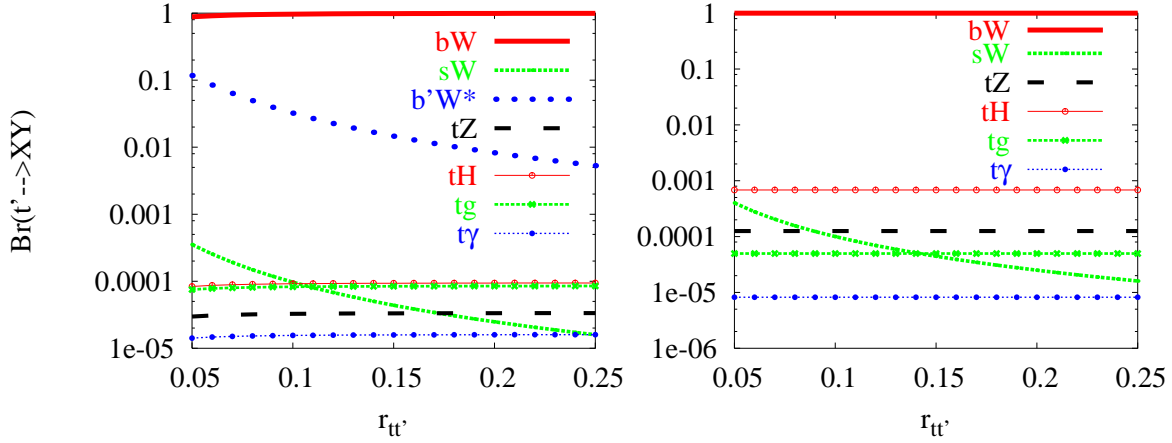


Figure 7: Same as Fig. 6 with $|V_{cb'}| = |V_{t's}| = 10^{-3}$.

above the $t' \rightarrow tg$ rate around 10^{-4} order. The $t' \rightarrow t\gamma$ mode is around 10^{-5} . The $t' \rightarrow tH$ rate may be measurable at the LHC, but the other rates may be more difficult.

For suppressed $|V_{t's}| \ll 0.04$, e.g. $|V_{t's}| \approx 10^{-3}$, $t' \rightarrow sW$ becomes suppressed. For $m_{b'} = 240$ GeV case shown in Fig. 7(a), $t' \rightarrow sW$ mode is of comparable size to the FCNC decay modes for $r_{tt'} \lesssim 0.08$, and drops lower for larger $r_{tt'}$. The other features, including FCNC, are not very sensitive to $V_{t's}$ and similar to Fig. 6(a). For $m_{b'} = 360$ GeV $> m_{t'} = 300$ GeV, as shown in Fig. 7(b), $t' \rightarrow b'W^*$ is forbidden, while the suppressed $t' \rightarrow sW$ mode drops below $t' \rightarrow tZ$ for $r_{tt'} \lesssim 0.1$. Otherwise the features are similar to Fig. 6(b).

Thus, the t' quark behaves like a heavy top quark, with $t' \rightarrow bW$ the dominant decay

mode. But the decay modes are still rather rich with $t' \rightarrow b'W^*$ and sW possibilities. Unlike the top, FCNC $t' \rightarrow tH, tZ, tg$ decays are around 10^{-4} , with $t' \rightarrow tH$ reaching branching ratio of the order 10^{-3} for $m_{b'} > m_{t'}$, while $t' \rightarrow t\gamma$ is of order a few 10^{-5} . The $t' \rightarrow tH, tZ$ rates may be measurable at the LHC.

5 FCNC $e^+e^- \rightarrow Q\bar{q} + \bar{Q}q$ Associated Production

There has been several studies looking for collider signatures of the FCNC top couplings, both at lepton colliders as well as at hadron colliders. To the best of our knowledge, there is no dedicated study of the associated production $e^+e^- \rightarrow Q\bar{q} + \bar{Q}q$, with Q - q being t - c , t' - t , b' - b or b - s . Because of the very large mass of the heavy quark Q , $Q\bar{q}$ production at an e^+e^- machine would have a clear signature [51]. The top-charm production at lepton colliders e^+e^- and $\mu^+\mu^-$ has been studied in two Higgs doublet models with and without Natural Flavor Conservation, the so called 2HDM-II and 2HDM-III, which can lead to measurable effects [51, 52, 53]. It has been pointed out that the tree level Higgs vertex $\phi\bar{t}c$ can be better probed through t -channel WW and/or ZZ fusion at high energy e^+e^- collisions $e^+e^- \rightarrow t\bar{c}\nu_e\bar{\nu}_e$ and $e^+e^- \rightarrow t\bar{c}e^+e^-$ [54, 55]. An interesting feature of those reactions is that, being t -channel, their cross sections grow with energy, unlike s -channel reactions $e^+e^- \rightarrow t\bar{c}$, which are suppressed at high energies. The cross sections of $e^+e^- \rightarrow t\bar{c}\nu_e\bar{\nu}_e$ and $e^+e^- \rightarrow t\bar{c}e^+e^-$ are found to be one or two orders of magnitude higher than the cross sections of $e^+e^- \rightarrow t\bar{c}$ [54, 55].

With the above possible probes to Higgs FCNC couplings in the backdrop, here we pursue the direct probe of FCNC in e^+e^- collisions. We have three sets of diagrams for $e^+e^- \rightarrow Q\bar{q}$ process: $e^+e^- \rightarrow \gamma^* \rightarrow Q\bar{q}$, $e^+e^- \rightarrow Z^* \rightarrow Q\bar{q}$, and box diagrams, as depicted in Fig. 8. Calculation of the full set of diagrams is done with the help of FormCalc [43]. We have checked both analytically and numerically that the result is ultraviolet (UV) finite and renormalization scale independent. We will present only unpolarized cross sections. It is well known that the cross sections for polarized initial states differ from the unpolarized cross sections only by a normalization factor.

In the present study, we limit ourselves to e^+e^- colliders. The cross sections for $e^+e^- \rightarrow Q\bar{q}$, if sizeable, can give information on the FCNC couplings $Q \rightarrow q\gamma$ and $Q \rightarrow qZ$ as well as on $Z \rightarrow s\bar{b}$. We shall first consider $e^+e^- \rightarrow b\bar{s}$ as it is the only one that can be probed in principle at the high luminosity SuperB factories, and also at a specialized Z factory. In the second subsection we will turn to the cases of $Q = t, b'$ and t' .

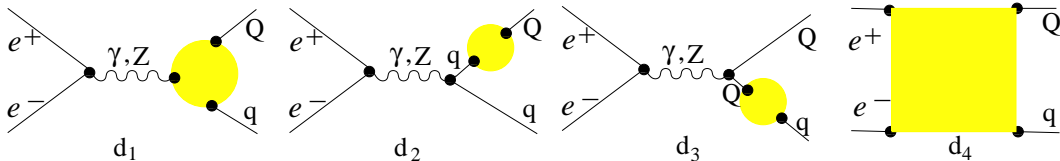


Figure 8: Topological contributions to $e^+e^- \rightarrow Q\bar{q}$.

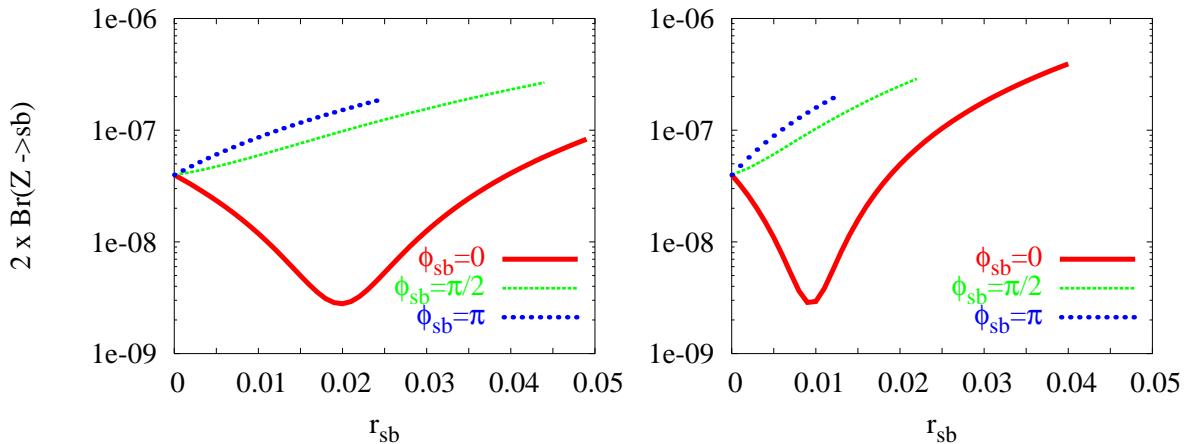


Figure 9: Fourth generation contribution to $\mathcal{B}(Z \rightarrow b\bar{s} + \bar{b}s)$ vs r_{sb} for $m_{t'} = 300$ GeV (left) and 400 GeV (right) for three values of $\phi_{sb} = 0, \pi/2, \pi$. The lines terminate when $B \rightarrow X_s l^+ l^-$ exceeds 2σ range from experimental value of $(6.1_{-1.8}^{+2.0}) \times 10^{-6}$.

5.1 $e^+e^- \rightarrow b\bar{s} + \bar{b}s$

As pointed in the Introduction, in SM the branching ratio for $Z \rightarrow b\bar{s} + \bar{b}s$ is of the order 10^{-8} . New physics contributions, like 2HDM and SUSY, to rare $Z \rightarrow b\bar{s} + \bar{b}s$ decay have been extensively studied [56, 57] and shown to enhance $\mathcal{B}(Z \rightarrow b\bar{s} + \bar{b}s)$. At LEP the sensitivity to rare Z decay is about 10^{-5} , while at future Linear Colliders operating at Z mass (e.g. GigaZ option of the TESLA LC) will bring this sensitivity up to the level of 10^{-8} [2]. It is then legitimate to look for new physics in rare Z decays. Ref. [57] considered effect of 2HDM-III together with 3 and 4 fermions generations. In this section we will consider effect of sequential fourth generation on rare Z decay using our parameterization described before and taking into account experimental constraints such as $B \rightarrow X_s \gamma$ and $B \rightarrow X_s l^+ l^-$.

The amplitude of such $b \rightarrow s$ transition is of the form given by Eq. (7). Like the case of $b \rightarrow s \gamma$, the CP phase ϕ_{sb} could play a crucial role. In Fig. 9 we illustrate fourth generation contribution to the branching ratio of $Z \rightarrow b\bar{s}$ as function of r_{sb} for $m_{t'} = 300$ GeV (left) and 400 GeV (right), and for three values of $\phi_{sb} = 0, \frac{\pi}{2}, \pi$. We allow $B \rightarrow X_s l^+ l^-$ to be in the 2σ range of the experimental value $(6.1_{-1.8}^{+2.0}) \times 10^{-6}$. Data points which do not satisfy this constraint are not plotted. One sees that $\mathcal{B}(Z \rightarrow b\bar{s})$ can reach 4×10^{-7} for $r_{sb} \approx 0.04$ and $m_{t'} = 400$ GeV. The observed dip in the plots correspond to destructive interference between t and t' contributions. This dip appears only for $\phi_{sb} = 0$, while for CP phase $\phi_{sb} \gtrsim \pi/2$ the t' contribution interferes constructively with the top which leads to a small enhancement of the rate (see Eq. (7)).

Off the Z peak, $e^+e^- \rightarrow \bar{b}s$ can still be probed at the future ILC. The cross section can be enhanced by about one order of magnitude with respect to SM cross section, depending on thresholds and the relative phase ϕ_{sb} , as illustrated in Fig. 10. The values of r_{sb} and

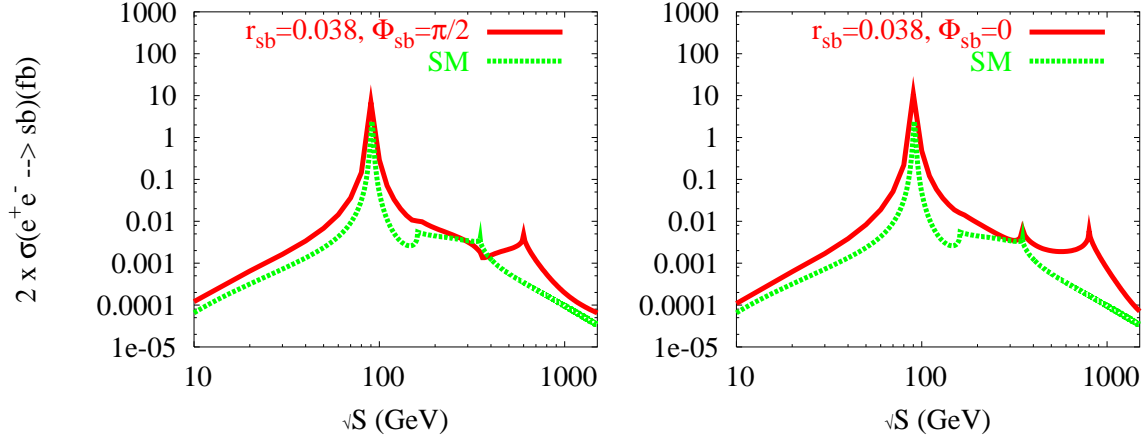


Figure 10: Fourth generation contribution to $e^+e^- \rightarrow s\bar{b} + \bar{s}b$ as a function of \sqrt{s} for $r_{sb} = 0.038$, $m_{t'} = 300$ GeV (left), 400 GeV (right).

ϕ_{sb} have been fixed such that $B \rightarrow X_s l^+ l^-$ is satisfied. In fact, we choose r_{sb} and ϕ_{sb} that saturate $\mathcal{B}(B \rightarrow X_s l^+ l^-)$. Near the Z pole $\sqrt{s} \approx M_Z$, the cross section can be larger than 10 fb and decreases when we increase the CM energy. One can reach ≈ 0.01 fb for $m_{t'} = 400$ GeV and $r_{sb} = 0.038$. There are several threshold effects which manifest themselves as small kinks in Fig. 10, corresponding to WW , tt and $t't'$ threshold production.

Motivated by the high luminosity accumulated by the B factories, e.g. about 500 fb^{-1} by Belle experiment at present, as well as the possibility for a future SuperB factory upgrade, we study the associated production of bottom-strange at center of mass energy $\sqrt{s} \simeq 10.6$ GeV both in SM and in SM with fourth generation. This is illustrated also in Fig. 10, which extends down to $\sqrt{s} = 10.6$ GeV. In SM one has about 10^{-4} fb which leads to negligible number of events at present B factories. With fourth generation contribution, the cross section for $e^+e^- \rightarrow \bar{b}s$ at $\sqrt{s} = 10.6$ GeV can be enhanced only mildly, largely due to $B \rightarrow X_s l^+ l^-$ constraint, and remains of the order 10^{-4} . But with several order of magnitude increase in luminosity at the SuperB factories, $e^+e^- \rightarrow \bar{b}s$ may become interesting.

5.2 $e^+e^- \rightarrow t\bar{c}, b'\bar{b}, t'\bar{t}$

Due to severe GIM cancellations between bottom, strange and down quarks as their masses are close to degenerate on the top scale, the SM cross section for $e^+e^- \rightarrow \bar{t}c$ is very suppressed. As one can see from Fig. 11(a), the $e^+e^- \rightarrow \bar{t}c$ cross section in SM is more than five orders of magnitude lower than the corresponding $e^+e^- \rightarrow \bar{b}s$ cross section in SM given in Fig. 10 at the same energy. The cross section is of order 10^{-9} fb, in agreement with [58]. For $e^+e^- \rightarrow \bar{b}s$ the internal fermions in SM are top, charm and up quarks. Because of the large top mass which is well split from the other internal quarks, the cross section for $e^+e^- \rightarrow \bar{b}s$ is in the range 10^{-4} – 10^{-2} fb for $\sqrt{s} \in [200, 1000]$ GeV as already discussed,

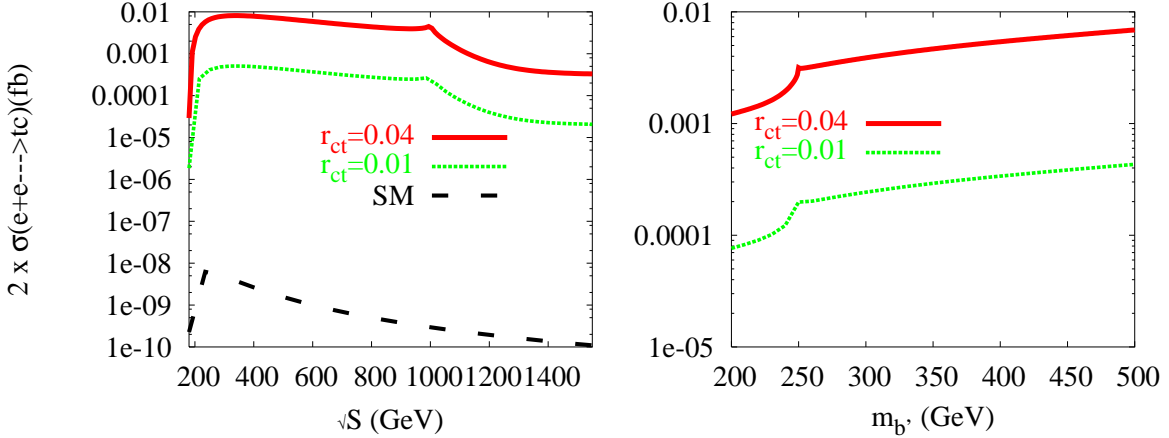


Figure 11: Fourth generation contribution to $e^+e^- \rightarrow t\bar{c} + \bar{t}c$ as a function of \sqrt{s} (left) for $m_{b'} = 500$ GeV, and as a function of $m_{b'}$ at $\sqrt{s} = 500$ GeV (right) and 2 values of r_{ct} . The SM cross section for $e^+e^- \rightarrow t\bar{c} + \bar{t}c$ is also shown in left plot.

and in agreement with [59].

The fourth generation b' quark can clearly affect the $e^+e^- \rightarrow \bar{t}c$ cross section significantly, as seen already in our discussion of $t \rightarrow cX$ decays. For sake of future ILC studies, we illustrate the cross section vs \sqrt{s} in Fig. 11(a) our numerical results for heavy $m_{b'} = 500$ GeV and several values of r_{ct} . We also show the sensitivity to $m_{b'}$ mass in Fig. 11(b). We see that the cross section for $e^+e^- \rightarrow \bar{t}c$ can get enhanced by six orders of magnitude with respect to the SM values. The cross section turns on sharply above threshold, becoming sizeable above $\sqrt{s} = 200$ GeV, and can reach values of ~ 0.01 fb for large $r_{ct} = 0.04$. One would still need a high luminosity of $\mathcal{L} \gtrsim 500$ fb $^{-1}$ or more to get at best a few events. Above $\sqrt{s} \gtrsim 1000$ GeV, the cross section decreases with increasing energy, reaching a value of $\approx 10^{-4}$ fb at $\sqrt{s} \gtrsim 1.5$ TeV. One can see a kink around $\sqrt{s} = 1000$ GeV in Fig. 11(a), which corresponds to threshold production of b' pair. In Fig. 11(b) we illustrate the dependence of $e^+e^- \rightarrow \bar{t}c$ cross section on b' mass for the more modest energy of $\sqrt{s} = 500$ GeV. At $m_{b'} = 250$ GeV, one can see a kink which corresponds to the threshold production of b' pair. For $r_{ct} = 0.04$ the cross section can be enhanced by one order of magnitude when varying $m_{b'}$ from 200 to 500 GeV.

By the same reason that $b' \rightarrow b$ and $t' \rightarrow t$ transitions have larger rates than $t \rightarrow c$ transitions, one expects $e^+e^- \rightarrow b'\bar{b}$ and $t'\bar{t}$ to have larger cross sections. If the fourth generation exists, it would be copiously produced at the LHC, and discovery is not a problem. For the future ILC, the simplest way to produce fourth generation Q is through Q pair production $e^+e^- \rightarrow \gamma^*, Z^* \rightarrow Q\bar{Q}$ if enough center of mass energy is available, i.e. $\sqrt{s} \gtrsim 2m_Q$. But the production of fourth generation Q in association with a lighter quark q , $e^+e^- \rightarrow Q\bar{q}$, would be kinematically better than $e^+e^- \rightarrow Q\bar{Q}$ pair production. It offers the possibility of searching for m_Q up to $\sqrt{s} - m_q$, in contrast to pair production which only probes up to $m_Q \lesssim \sqrt{s}/2$.

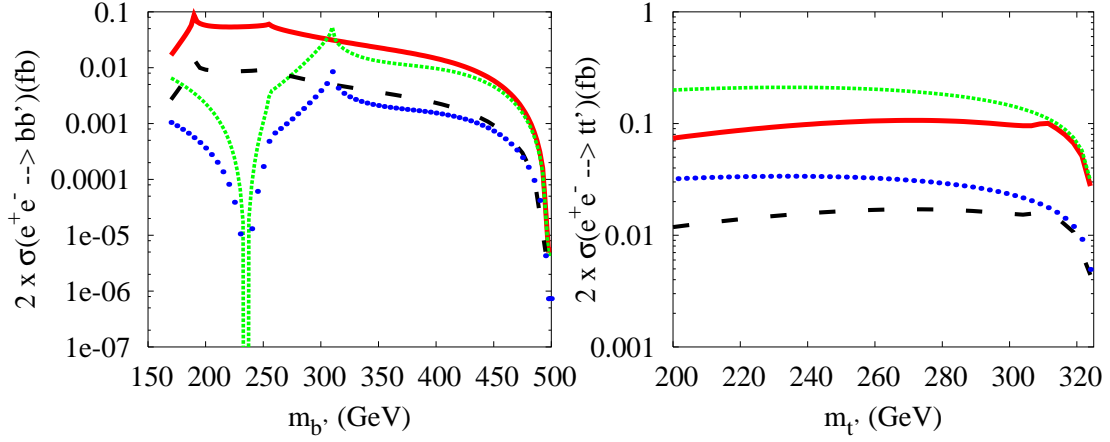


Figure 12: Fourth generation contribution to $e^+e^- \rightarrow b\bar{b}'$ as a function $m_{b'}$ (left), and $e^+e^- \rightarrow t\bar{t}'$ as a function of $m_{t'}$ (right) at $\sqrt{s} = 500$ GeV. $r_{bb'} = 0.25$ for solid and small dash plots and $r_{bb'} = 0.1$ for long dash and dots plots. $m_{t'} = m_{b'} + \Delta$ GeV with $\Delta = 60$ GeV for solid and long dash and -60 GeV for the other plots

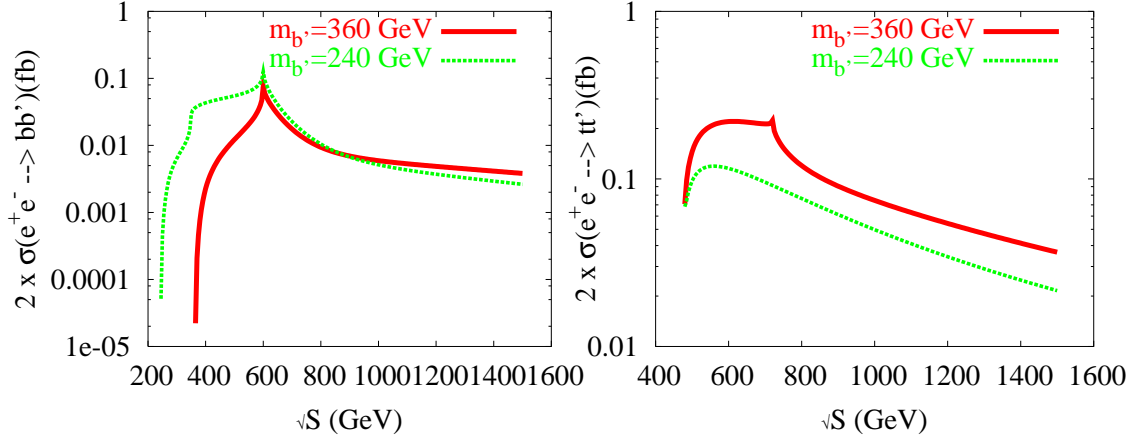


Figure 13: $\sigma(e^+e^- \rightarrow b\bar{b}')$ (left) and $\sigma(e^+e^- \rightarrow t\bar{t}')$ (right) as a function \sqrt{s} for $r_{bb'} = r_{tt'} = 0.25$, $m_{t'} = 300$ GeV and $m_{b'}$ as indicated

In Fig. 12, we present cross sections for both $e^+e^- \rightarrow b\bar{b}'$ (left) and $t\bar{t}'$ (right) at $\sqrt{s} = 500$ GeV, as functions of $m_{b'}$ and $m_{t'}$, respectively. Obviously, the largest $r_{bb'}$ (or $r_{tt'}$) gives the largest cross section. We have illustrated both cases with $m_{t'} = m_{b'} \pm 60$ GeV. In the case where $m_{t'} = m_{b'} + 60$ GeV $> m_{b'}$, this explains the kink at $m_{b'} = 190$ GeV in Fig. 12(a), which corresponds to the opening of the $t\bar{t}'$ threshold, and a slight kink at $m_{b'} = 255$ GeV, which corresponds to the $b' \rightarrow tW$ cut. While in the case $m_{t'} = m_{b'} - 60$ GeV $< m_{b'}$, it's clear that for $m_{b'} = 235$ GeV which corresponds to $m_{t'} = 175$ GeV $= m_t$ there is a GIM cancellation, while the kink around $m_{b'} \approx 310$ GeV corresponds to the

opening of the $t'\bar{t}'$ threshold. Above $m_{b'} \approx 250$ GeV, $b'\bar{b}'$ pair production no longer occurs, but $e^+e^- \rightarrow b\bar{b}'$ can still be probed, with cross section of order a few 0.01 fb. Analogously, as seen in Fig. 12(b), the cross section for $e^+e^- \rightarrow t\bar{t}'$ remains more or less constant around 0.2 fb, even when $t'\bar{t}'$ pair production is forbidden. Of course, the possibilities are richer as $m_{b'}$ and $m_{t'}$ are unknown, but in both $e^+e^- \rightarrow b\bar{b}'$ and $e^+e^- \rightarrow t\bar{t}'$ cases, it is clear that for large $r_{bb'} \sim 0.2$, the cross sections can be larger than 0.01 fb, reaching 0.1 fb, which could lead to a few ten events for the high luminosity option $\mathcal{L} \gtrsim 500 \text{ fb}^{-1}$.

For completeness, we show in Fig. 13 cross sections for both $e^+e^- \rightarrow b\bar{b}'$ (left) and $t\bar{t}'$ (right) for $m_{t'} = 300$ GeV, $m_{b'} = 240, 360$ GeV and large $r_{bb'} = r_{tt'} = 0.25$ as functions of center of mass energy, respectively. It is clear from Fig. 13 that the associate production $e^+e^- \rightarrow b\bar{b}'$ or $e^+e^- \rightarrow t\bar{t}'$ can lead to a few ten of event before one can accumulate enough energy to produce a pair of b' or t' . Thus, one can not only study FCNC $b' \rightarrow bZ$ and $t' \rightarrow tX$ decays at the ILC, one could also probe FCNC induced associated $b'\bar{b}'$ and $t'\bar{t}'$ production.

6 Discussion

At the Tevatron or the LHC, fourth generation b' and t' quarks can be pair produced through gg fusion and $q\bar{q}$ annihilation, with the same sizeable QCD cross section for a given mass. For example, at Tevatron, for $\sqrt{s} = 2$ TeV and a heavy quark $m_Q = 240$ GeV, one can have a non-negligible cross section of the order ≈ 1.2 pb. At the LHC the cross section can increase by about 2 orders of magnitude, with much higher luminosity. Consequently, discovering the fourth generation is not a problem for hadronic machines, and we are on the verge of finally discovering the fourth generation, or ruling it out conclusively. The search strategy would depend on decay pattern, and once discovered, the ILC may be needed for precise measurements of all sizable decay modes.

We are concerned with heavy fourth generation $m_{b'}, m_{t'} \gtrsim 200$ GeV. The allowed tree level decays of the b' are $b' \rightarrow cW$ (ignoring uW), $tW^{(*)}$, and $t'W^*$ if kinematically possible, and of course our main interest of FCNC decays $b' \rightarrow bZ, bH, bg, b\gamma$, and the suppressed $b' \rightarrow sZ, sH, sg, s\gamma$ (see Appendix). Similarly, the allowed t' tree level decays are $t' \rightarrow sW, bW$ (dropping again dW), $b'W^*$ and the loop-induced FCNC decays $t' \rightarrow tZ, tH, tg, t\gamma$ and $t' \rightarrow cZ, cH, cg, c\gamma$. The relative weights of these decays have been surveyed in Section 4, and the prognosis is that FCNC decays can be measured at the LHC, once the fourth generation is discovered. Here we offer some discussion on various special situations.

6.1 Comment on Tevatron Run-II

For $m_t + M_W > m_{b'} > M_Z + m_b$ and if $V_{cb'}$ is suppressed, the decay $b' \rightarrow bZ$ [48] is expected to dominate over the other FCNC decay processes, except for $b' \rightarrow bH$ [46, 49] if $m_{b'} > M_H + m_b$ also. The CDF Collaboration [28] gave an upper limit on the product $\sigma(p\bar{p} \rightarrow b'\bar{b}') \times [\mathcal{B}(b' \rightarrow bZ)]^2$ as a function of $m_{b'}$, which excludes at 95% CL the range

$100 \text{ GeV} < m_{b'} < 199 \text{ GeV}$ if $\mathcal{B}(b' \rightarrow bZ) = 100\%$. For $\mathcal{B}(b' \rightarrow bH) \neq 0$, so long that $\mathcal{B}(b' \rightarrow bZ)$ does not vanish, the CDF bound still largely applies since hadronic final states of $b' \rightarrow bZ$ and bH are rather similar, and in fact the bH mode has better b -tagging efficiency.

What CDF apparently did not pursue in any detail is the $b' \rightarrow cW$ possibility. Nor has the complicated case of $b' \rightarrow tW^*$ been much discussed. Clearly the b -tagging efficiency for cW mode would be much worse than bZ or bH . Since b -tagging is an important part of the CDF $b' \rightarrow bZ$ search strategy, the CDF search may be evaded if $\mathcal{B}(b' \rightarrow cW)$ is sizable. As we have demonstrated in Fig. 2, $b' \rightarrow cW$ can be the dominant decay mode for $m_{b'} = 240 \text{ GeV}$ for all range of $r_{bb'}$, if $V_{cb'}$ could be as sizable as $V_{cb} \simeq 0.04$. However, in case $V_{cb'}$ is rather suppressed, FCNC decays like $b' \rightarrow bZ, bH$ can compete with $b' \rightarrow cW, tW^*$. Hence, more generally one should make a combined search for $b' \rightarrow cW, bZ$ and bH [31], even tW^* . On the other hand, t' could turn out to be lighter than b' . In this case one expects top-like decay pattern, and one can look for $t' \rightarrow bW$, but $t' \rightarrow sW$ could also be sizable, again diluting the effectiveness of b -tagging.

We stress that, for either the case of sizable $b' \rightarrow cW$ or $t' \rightarrow sW$, the possible loss of b -tagging efficiency should be kept in mind in heavy quark search. Although one may face more background because of this, the possibility of dominant or prominent FCNC $b' \rightarrow bZ, bH$ should continue to be pursued in the closing years of Tevatron Run-II.

6.2 Large or Small $V_{cb'}$ ($V_{t's}$)?

The CKM matrix becomes 4×4 in case of four generations. Since the elements $V_{ud}, V_{us}, V_{cd}, V_{cb}, V_{cs}, V_{ub}$, in that order, are suitably well measured, one can continue to use the usual three generation parameterization. The additional 3 mixing angles and 2 CP phases, following Ref. [36], are placed in $|V_{t'b}|, |V_{t's}|, |V_{t'd}|$, and $\arg(-V_{t's}), \arg(-V_{t'd})$. Without much loss of generality for future heavy quark search and studies, we have dropped $V_{t'd}$, as well as $V_{ub'}$ [60]. It is nontrivial that we already have a bound on $|V_{t'b}|$, as given in Eq. (5). Thus, the main unknown for our purpose is the angle and phase in $V_{t's}$ (which is closely related to $V_{cb'}$). This element could impact on $b \rightarrow s$ transitions if sizable.

Large $V_{t's}$ Scenario

There are two recent hints of New Physics in $b \rightarrow s$ transitions. One is the difference, called $\Delta\mathcal{S}$, between the time-dependent CP violation measured in penguin dominant $b \rightarrow s\bar{s}s$ modes such as $B \rightarrow \phi K_S$, and tree dominant $b \rightarrow c\bar{c}s$ modes such as $B \rightarrow J/\psi K_S$. Three generation SM predicts $\Delta\mathcal{S} \cong 0$ [61], but measurements at B factories persistently give $\Delta\mathcal{S} < 0$ [21] in many modes, though they are not yet statistically significant. The other indication is the difference in direct CP violation measured in $B \rightarrow K^+\pi^-$ vs $K^+\pi^-$ modes [21], $\mathcal{A}_{K^+\pi^0} - \mathcal{A}_{K^+\pi^-} \neq 0$. Although this could be due to hadronic effects such as enhancement of so-called ‘‘color-suppressed’’ amplitude, the other possibility could be New Physics in the electroweak penguin amplitude. It has been shown that the fourth generation contribution to EW penguin with large $V_{t's}^* V_{t'b}$ and near maximal CP phase [20]

could explain the effect. It is consistent with B , K and D data, and predicts enhanced $K_L \rightarrow \pi^0 \nu \bar{\nu}$ decay [35]. Assuming $m_{t'} = 300$ GeV, it turns out that large $V_{t's}^* V_{t'b} \approx 0.025$ with large phase is allowed, while $|V_{t's}|$ is only slightly smaller than $|V_{t'b}|$. It further gives rise to the downward trend of $\Delta\mathcal{S} < 0$ observed at B factories, though not quite sufficient in strength [22]. Thus, it could in principle account for both hints of New Physics. As we have demonstrated, after taking into account $b \rightarrow sl^+l^-$ constraint, $Z \rightarrow sb$ is only slightly enhanced. But Ref. [20] predicts large and negative CP violation in B_s mixing, which can be probed at the Tevatron Run-II, and can be definitely measured by LHCb at the LHC shortly after turn-on.

For our purpose of heavy quarks decays, taking $V_{t'b} \simeq -0.22$, Ref. [35] finds

$$\begin{aligned} V_{cb'} &\simeq 0.12 e^{i66^\circ}, & V_{t's}^* &\simeq -0.11 e^{i70^\circ}, & V_{tb'} &\simeq 0.22 e^{-i1^\circ}, \\ V_{t's}^* V_{t'b} &\equiv r_{sb} e^{i\phi_{sb}} \simeq 0.025 e^{i70^\circ}, & V_{cb'} V_{tb'}^* &\equiv r_{ct} e^{i\phi_{ct}} \simeq 0.025 e^{i67^\circ}, \\ V_{t'b}^* V_{t'b'} &\equiv r_{bb'} \simeq -0.21, & V_{tb'} V_{t'b'}^* &\equiv r_{tt'} \simeq 0.21 e^{-i1^\circ}. \end{aligned} \quad (20)$$

Thus, $V_{cb'}$ and $V_{t's}$ are even larger than the 0.04 value used in Figs. 4 and 6. If the scenario is realized, $b' \rightarrow cW$ would predominate for $m_{b'} \lesssim m_{t'}$, and even for $m_{b'} > m_{t'}$, $b' \rightarrow cW$ would be comparable to $b' \rightarrow tW$. The relative FCNC rates would be slightly reduced, but still measurable. The suppressed $b' \rightarrow sX$ decays discussed in Appendix may become interesting. Since the $\Delta\mathcal{S}$ and $\mathcal{A}_{K^+\pi^0} - \mathcal{A}_{K^+\pi^-} \neq 0$ problems may soften, we have only presented the $V_{cb'} \approx V_{cb} \approx 0.04$ case in Figs. 4 and 6.

Very Suppressed $|V_{cb'}| \approx |V_{t's}|$ Scenario

The measured three generation quark mixing elements exhibit an intriguing pattern of $|V_{ub}|^2 \ll |V_{cb}|^2 \ll |V_{us}|^2 \ll 1$. In the four generation scenario of Ref. [20, 35], this pattern is violated by the strength of $|V_{cb'}|^2$ in Eq. (20) being an order of magnitude larger than $|V_{cb}|^2$. This is in itself not a problem, since the CKM mixing elements are parameters of the SM, and are *a priori* unknown. The $b \rightarrow s$ transitions may well hold surprises for us.

It may also happen that the hints for New Physics in $b \rightarrow s$ transitions eventually evaporate. For that purpose, we have shown the other end of very suppressed $|V_{cb'}| \approx |V_{t's}| \approx 10^{-3}$. Part of the reason for choosing such a small value is because, for $m_{b'} \lesssim 200$ GeV which is well within reach of the Tevatron, it has been extensively discussed in Refs. [31, 46]. It has been shown that, if we take the ratio $|V_{cb'}|/(V_{t'b'} V_{t'b}^*)$ to be of the order 10^{-3} , then the tree level $b' \rightarrow cW$ decay and the loop level $b' \rightarrow bZ, bH$ decays could be comparable, and the CDF bound can be relaxed. As seen in Figs. 5 and 7, for even smaller $V_{cb'}$, the $b' \rightarrow cW$ and $t' \rightarrow sW$ decays become rare decays. This is analogous to tree dominant $b \rightarrow u$ decays such as $B \rightarrow \pi^+\pi^-$ being weaker than loop induced $b \rightarrow s$ decays such as $B \rightarrow K^+\pi^-$.

For very small $V_{cb'}$ (with $V_{ub'}$ already assumed small), one effectively has the 2×2 structure between the two $(t, b)_L$ and $(t', b')_L$ doublets, with the mixing element $V_{t'b} \cong -V_{tb'}$ controlling both the tree level and loop induced decays. The phenomenology has already been considered in Section 4. In general one expects $b' \rightarrow tW$ and $t' \rightarrow bW$ to be dominant,

with FCNC rates at 10^{-4} to 10^{-2} level. The exception is when $m_{b'} \lesssim m_t + M_W$, so $b' \rightarrow tW^*$ gets kinematically suppressed, as illustrated in Fig. 5(a). This “FCNC dominance” scenario is precisely the domain that is relevant for Tevatron Run-II stressed in previous subsection. Whether Tevatron explores this domain further or not, it would be fully covered by the LHC.

The discovery of FCNC dominance for a *heavy* quark would be truly amusing.

7 Conclusions

The study of flavor changing neutral couplings involving s and b quarks has yielded a most fruitful program in the past 40 years, and is still going strong. With the turning on of the LHC approaching, we will soon enter an era of studying FCNC involving genuine heavy quarks, starting with the top. The (three generation) SM predictions for $t \rightarrow cX$ where $X = Z, H, g$ and γ are orders of magnitude below sensitivity. This implies an enormous range of probing for beyond SM(3) effects.

With the top quark as the single heavy quark at the weak scale, it may be useful to contemplate additional heavy quarks such as a sequential fourth generation. Unfortunately, we find that virtual effects from b' still cannot enhance $t \rightarrow cX$ to within sensitivity at LHC, once $b \rightarrow s$ constraints are imposed. In the case of $Z \rightarrow \bar{s}b$, again because of $b \rightarrow s$ constraints, we find $\mathcal{B}(Z \rightarrow sb)$ can only reach 10^{-7} . This at best can be probed in the distance future at a specialized GigaZ.

The decay of fourth generation b' and t' quarks themselves are far more promising. We have studied both the CC decays as well as the FCNC decay modes. We have shown that there is a rather broad range of possibilities for b' decay, depending on $m_{b'}$, $V_{cb'}$ and $V_{tb'}$. For $m_{b'} \lesssim 240$ GeV and very small $V_{cb'}$, FCNC dominance is possible. In general, FCNC $b' \rightarrow bZ, bH$ decays could compete with $b' \rightarrow cW$ and tW^* , and should be of interest at the Tevatron Run-II. For sizable $V_{cb'}$ values, the $b' \rightarrow cW$ mode would dominate, which would greatly affect the effectiveness of b -tagging for heavy quark search. For $m_{b'} > m_t + M_W$, the dominance of $b' \rightarrow tW$ implies $b'\bar{b}' \rightarrow t\bar{t}W^+W^- \rightarrow b\bar{b}W^+W^+W^-W^-$, or $4W$ s plus 2 b -jets, which should be of interest at LHC. Except for the case of small $V_{cb'}$ and light $m_{b'}$, the FCNCs are typically at 10^{-4} – 10^{-2} order hence always within reach at the LHC, even though the signals may vary in richness and complexity.

The t' case is simpler. Basically $t' \rightarrow bW$ dominates, so it acts as a heavy top. In principle, $t' \rightarrow sW$ could cut in and dilute b -tagging effectiveness, but that would require a rather large $V_{t's}$ compared to $V_{t'b}$. The good news is that FCNC rates are again in the accessible range at the LHC, with $t' \rightarrow tH$ possibly reaching up to 10^{-3} .

We have also studied the direct production through FCNC, $e^+e^- \rightarrow q\bar{Q}$, at the future ILC. Unfortunately, these are not very prominent. The $e^+e^- \rightarrow \bar{s}b$ and $\bar{c}t$ are below sensitivity, while $e^+e^- \rightarrow \bar{b}b', \bar{t}t'$ would yield not more than a few ten events. Clearly, these numbers would be better clarified once the fourth generation is discovered at the LHC.

We conclude that Tevatron Run-II should be able to probe the light b' (and t' as well) case, where FCNC could be most prominent. The LHC, however, should be able to

establish the fourth generation beyond any doubt, if it exists. Furthermore, the LHC has the capability to measure all the $b' \rightarrow bZ, bH, bg, b\gamma$ as well as $t' \rightarrow tZ, tH, tg, t\gamma$ decays and offer a wealth of information. These modes could then be studied in further detail at the ILC. Alternatively, the fourth generation could *finally* be put to rest by the LHC.

Acknowledgements

AA is supported by the Physics Division of National Center for Theoretical Sciences under a grant from the National Science Council of Taiwan. The work of WSH is supported in part by NSC-94-2112-M-002-035. We are grateful to A. Soddu for bringing Ref. [16] to our attention.

A Suppressed FCNC b' and t' Decays

The branching ratios for both the FCNC $b' \rightarrow bX$ and $t' \rightarrow tX$ transitions are considerably larger than the corresponding $t \rightarrow cX$ transitions, and should be observable at the LHC. This comes about because they involve $r_{bb'} = V_{t'b}^* V_{t'b'}$ and $r_{tt'} = V_{tb'} V_{t'b}^*$, which are larger than $r_{ct} = V_{cb'} V_{tb'}^*$ for $t \rightarrow cX$ transitions. The leading tree level decays are controlled by $V_{(c)tb'}$, $V_{t'b}$ and V_{tb} , respectively, which further suppress the FCNC $t \rightarrow cX$ branching ratios. That is, the tree level $t \rightarrow bW$ decay is unsuppressed, while loop induced FCNC $t \rightarrow cX$ decays are CKM suppressed. Having the decaying particles b' and t' heavier than the top quark also helps the respective b' and t' loop processes.

For both b' and t' , there are CKM suppressed FCNC decays as well. We consider $b' \rightarrow sX$ and $t' \rightarrow cX$ transitions. The unitarity relations are $\Sigma V_{is}^* V_{ib'} = 0$, and $\Sigma V_{cj}^* V_{tj} = 0$, respectively. For the loop amplitudes, however, since to good approximation u and c , as well as d , s and b , are practically degenerate on the b' , t' , t scale, we can take

$$V_{us}^* V_{ub'} + V_{cs}^* V_{cb'} = -(V_{ts}^* V_{tb'} + V_{t's}^* V_{t'b'}), \quad (21)$$

$$V_{cd} V_{t'd}^* + V_{cs} V_{t's}^* + V_{cb} V_{t'b}^* = -V_{cb'} V_{t'b'}^*. \quad (22)$$

The loop amplitudes for $b' \rightarrow s$ and $t' \rightarrow c$ transitions can then be expressed to good approximation as

$$\mathcal{M}_{b' \rightarrow s} \propto V_{ts}^* V_{tb'} [f(m_t) - f(0)] + V_{t's}^* V_{t'b'} [f(m_{t'}) - f(0)], \quad (23)$$

$$\mathcal{M}_{t' \rightarrow c} \propto V_{cb'} V_{t'b'}^* [f(m_{b'}) - f(0)]. \quad (24)$$

Comparing Eq. (24) with Eq. (13), the difference between $t' \rightarrow c$ and $t' \rightarrow t$ is just in the CKM factor $V_{tb'}$ and $V_{cb'}$, plus the kinematic difference of having a light c vs a heavy t in the final state (thus, the functions $f(x)$ are different). For $b' \rightarrow s$ compared to $b' \rightarrow b$, things are more complicated, and is more interesting. Eq. (12) should have had the same form as Eq. (23), but was simplified by the observation that $|V_{ub}^* V_{ub'}| \ll 1$ and $|V_{cb}^* V_{cb'}| \ll 1$ are likely, so one has $V_{tb}^* V_{tb'} \approx -V_{t'b}^* V_{t'b'}$, and the light quark contribution can

be ignored. In Eq. (23), however, one cannot ignore the light quark effect, which provides the proper GIM subtraction for the t and t' contributions. It is interesting to stress that both the CKM coefficients $V_{ts}^*V_{tb'}$ and $V_{t's}^*V_{t'b'}$ have nontrivial CP phases, which should be in principle different. The phase difference, together with possible absorptive parts of the loop functions $f(m_t) - f(0)$ and $f(m_{t'}) - f(0)$, can lead to CP violation, such as $b' \rightarrow sX$ vs $\bar{b}' \rightarrow \bar{s}X$ partial rate differences.

We illustrate first in Fig. 14 the simpler case of the decay widths of $t' \rightarrow c$ transitions normalized to $|V_{cb'}|^2$, as a function of $m_{b'}$ and $m_{t'}$. Comparing Fig. 14 with Fig. 3, it is clear that the partial widths $\Gamma(t' \rightarrow cX)/|V_{cb'}|^2$ are slightly larger than $\Gamma(t' \rightarrow tX)/r_{tt'}^2$. The reason is that $t' \rightarrow t$ transitions are more suppressed by phase space. As one can see from Fig. 3(b), $t' \rightarrow tZ$ and $t' \rightarrow tH$ are open only if $m_{t'} > m_t + m_Z$ and $m_{t'} > m_t + m_H$. It is useful to compare with the decay branching ratios given in Fig. 6 for $|V_{cb'}| \simeq |V_{t's}| \simeq 0.04$. The branching ratio for $t' \rightarrow cZ$ is about 0.00023 times the branching ratio of $t' \rightarrow sW$ in Fig. 6(a), with $t' \rightarrow cH$ (cg) just below (above), and $t' \rightarrow c\gamma$ is another factor of 3 lower. In Fig. 6(b), the branching ratios for $t' \rightarrow cH \gtrsim t' \rightarrow cZ$ is about 0.001 times the branching ratio of $t' \rightarrow sW$, with $t' \rightarrow cg$ slightly below, and $t' \rightarrow c\gamma$ another order of magnitude lower. Depending on $r_{tt'} = V_{tb}V_{t'b'}^*$, the $t' \rightarrow cX$ modes could be comparable to the $t' \rightarrow tX$ modes. For the HNS scenario [20, 35], where $r_{tt'}$ is not much larger than $|V_{cb'}|$, the $t' \rightarrow cX$ modes could dominate over $t' \rightarrow tX$ transitions. On the other hand, if $V_{cb'} \simeq 10^{-3}$ i.e. the case of Fig. 7, then $t' \rightarrow c$ transitions should be much suppressed compared to the $t' \rightarrow tX$ modes.

Thus, as one searches for FCNC $t' \rightarrow tX$ modes, the FCNC $t' \rightarrow cX$ modes should not be ignored. The latter modes have the advantage of being simpler.

For the case of $b' \rightarrow sX$, Eq. (23) has both t and t' loop contributions, which depend on the CKM elements $V_{ts}^*V_{tb'}$ and $V_{t's}^*V_{t'b'}$, respectively. These elements are not the same as the elements $V_{ts}^*V_{tb}$ and $V_{t's}^*V_{t'b}$ that enter $b \rightarrow s$ transitions discussed in Section 2. A

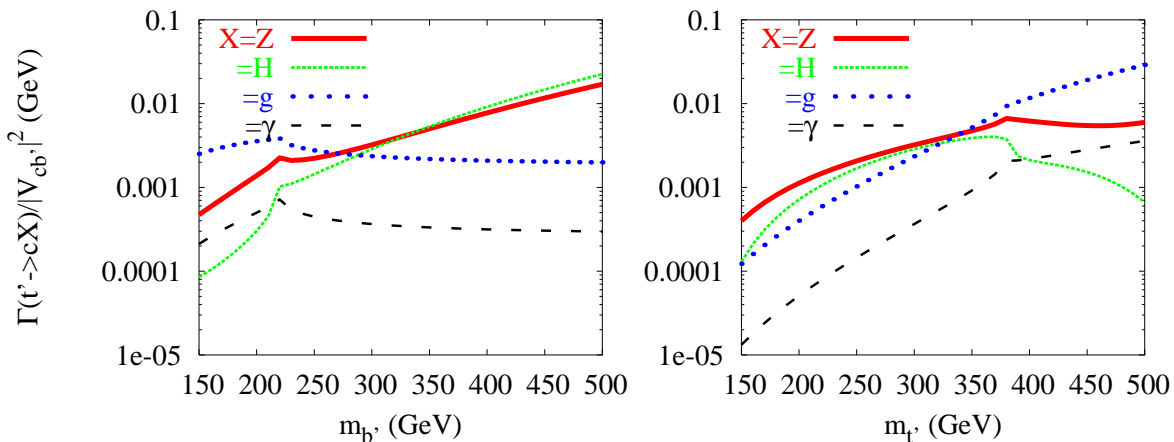


Figure 14: Decay width of $\Gamma(t' \rightarrow c\{Z, H, g, \gamma\})$ normalized to $V_{cb'}^2$, as a function of $m_{b'}$ for $m_{t'} = 300$ GeV (left), and as a function of $m_{t'}$ for $m_{b'} = 300$ GeV (right).

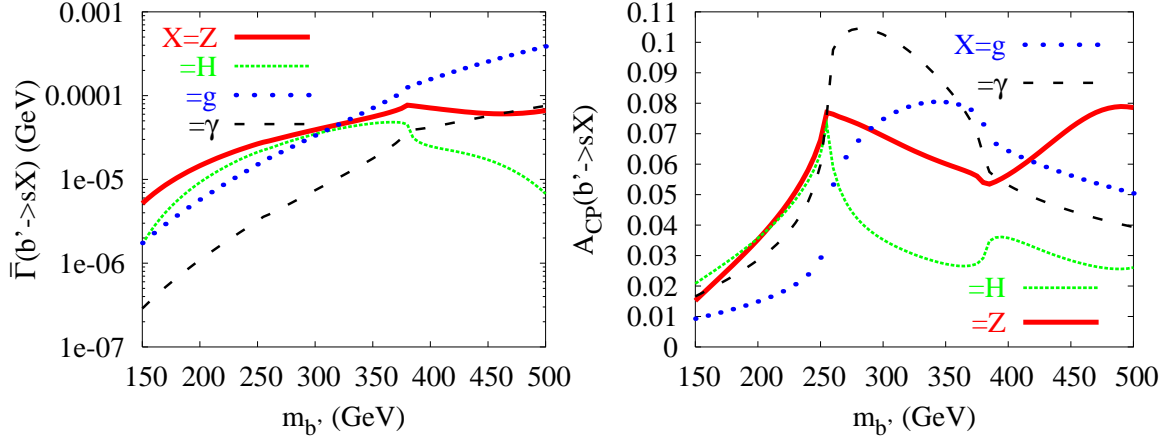


Figure 15: (Left) Decay width $\bar{\Gamma}(b' \rightarrow sX)$ and \mathcal{A}_{CP} for $b' \rightarrow sX$ (right) as a function of $m_{b'}$ for $m_{t'} = 300$ GeV in the HNS scenario.

detailed analysis would necessarily involve all the low energy $b \rightarrow s$, $s \rightarrow d$, $b \rightarrow d$ and $c \rightarrow u$ transitions, and is clearly beyond the scope of the present paper. Such an analysis has been performed in the HNS scenario [20, 35], which is motivated by the direct CP violation problem in $B \rightarrow K^+\pi^-$ vs $K^+\pi^0$ modes, and is discussed briefly in Sec. 6.2. It can further give [22] $\Delta\mathcal{S} < 0$ seen in many modes at the B factories. The $b' \rightarrow sX$ processes deserve further study, however, since they can exhibit CP violation in *very* heavy quark decays. To illustrate this, we will evaluate the average partial decay width of $b' \rightarrow sX$ defined as

$$\bar{\Gamma}(b' \rightarrow sX) = \frac{1}{2} \left(\Gamma(b' \rightarrow sX) + \Gamma(\bar{b}' \rightarrow \bar{s}X) \right), \quad (25)$$

and the CP asymmetry defined as

$$\mathcal{A}_{CP}(b' \rightarrow sX) = \frac{\Gamma(b' \rightarrow sX) - \Gamma(\bar{b}' \rightarrow \bar{s}X)}{\Gamma(b' \rightarrow sX) + \Gamma(\bar{b}' \rightarrow \bar{s}X)}. \quad (26)$$

Since $V_{ts}^*V_{tb'}$ and $V_{t's}^*V_{t'b'}$ would in general have different CP violating phase, while the corresponding CP conserving phases in $f(m_t) - f(0)$ and $f(m_{t'}) - f(0)$ could also be different, we expect $\mathcal{A}_{CP}(b' \rightarrow sX) \neq 0$.

We use the HNS scenario as illustration, where we find [35]

$$V_{ts}^*V_{tb'} = -0.012 e^{i24^\circ}, \quad V_{t's}^*V_{t'b'} = -0.11 e^{i70^\circ}. \quad (27)$$

From this we expect that the size of CP violation will be of the order $|V_{ts}^*V_{tb'}/V_{t's}^*V_{t'b'}| \approx 0.11$ or less. We illustrate in Fig. 15 the average decay width $\bar{\Gamma}(b' \rightarrow sX)$ and CP asymmetry $\mathcal{A}_{CP}(b' \rightarrow sX)$ as a function of $m_{b'}$. Note that the HNS scenario fixes $m_{t'}$ to 300 GeV, but the analysis is almost independent of $m_{b'}$. Comparing Fig. 15(a) and Fig. 14(b), we

see that, up to an overall factor, they are rather similar. This is because in the HNS scenario, the $V_{t's}^* V_{t'b'}$ term, i.e. the second term of Eq. (23), is dominant. This term is rather similar to Eq. (24) with $m_{b'} \leftrightarrow m_{t'}$. In fact, for Higgs and gluon final state, they should be identical. Even for the Z and γ final state, as seen from Fig. 15(a), the difference is minor.

Of course, it is the presence of the first t contribution term of Eq. (23), which interferes with the second t' contribution term, that makes CP violation possible. As expected, from Fig. 15(b) we see that the CP asymmetries for the $b' \rightarrow sX$ transitions are in the range of a few % up to 10%. For light $m_{b'} \approx 150 - 200$ GeV, \mathcal{A}_{CP} is rather small because $f(m_t) - f(0)$ and $f(m_{t'}) - f(0)$ have approximately similar phase. The asymmetries rise with $m_{b'}$ as the $b' \rightarrow tW$ threshold is approached. Passing this threshold, the asymmetries for the $b' \rightarrow sZ$ and sH modes start to drop, but continue to rise for the $b' \rightarrow sg$ and $s\gamma$ modes. Crossing the $b' \rightarrow t'W$ threshold, however, the asymmetries for the $b' \rightarrow sg$ and $s\gamma$ modes start to drop. The asymmetry for the $b' \rightarrow sZ$ starts to rise again, but for the $b' \rightarrow sH$ mode, it drops after rising briefly.

To conclude, $b' \rightarrow sX$ rates could be comparable to $b' \rightarrow bX$ if $V_{t's}^* V_{t'b'}$ is not much smaller than $V_{t'b}^* V_{t'b'}$, which is the case for the HNS scenario. The HNS scenario, however, is not optimized for CP violation effect in $b' \rightarrow sX$ modes. As the rates for these modes drop with the strength of $V_{t's}$, much larger CP violation effects could be possible. The phenomena seem rich and deserve further study, which we refer to a future work.

References

- [1] M. Beneke, I. Efthymipoulos, M.L. Mangano, J. Womersley (conveners) *et al.*, report in the *Workshop on Standard Model Physics (and more) at the LHC*, Geneva, hep-ph/0003033.
- [2] J.A. Aguilar-Saavedra *et al.* [ECFA/DESY LC Physics Working Group Collaboration], hep-ph/0106315; K. Abe *et al.* [ACFA Linear Collider Working Group], hep-ph/0109166; T. Abe *et al.* [American Linear Collider Working Group], in *Proc. of the APS/DPF/DPB Summer Study on the Future of Particle Physics (Snowmass 2001)* ed. N. Graf, hep-ex/0106055; hep-ex/0106056; hep-ex/0106057; hep-ex/0106058. For current developments, see <http://www.linearcollider.org/cms/>.
- [3] G. Eilam, J.L. Hewett and A. Soni, Phys. Rev. D **44** (1991) 1473 [Erratum-ibid. D **59** (1999) 039901].
- [4] B. Mele, S. Petrarca and A. Soddu, Phys. Lett. B **435**, 401 (1998).
- [5] F. Abe *et al.* [CDF Collaboration], Phys. Rev. Lett. **80**, 2525 (1998); M. Paulini [CDF and D0 Collaborations], hep-ex/9701019. D.W. Gerdes, hep-ex/9706001.
- [6] V.F. Obraztsov, *Prepared for 30th International Conference on High-Energy Physics (ICHEP 2000), Osaka, Japan, 27 Jul - 2 Aug 2000*; R. Barate *et al.* [ALEPH Collaboration], CERN-EP-2000-102.

- [7] J.A. Aguilar-Saavedra and G.C. Branco, Phys. Lett. B **495**, 347 (2000); J.A. Aguilar-Saavedra, Phys. Lett. B **502**, 115 (2001).
- [8] J.A. Aguilar-Saavedra, Acta Phys. Polon. B **35**, 2695 (2004).
- [9] S. Eidelman *et al.* [Particle Data Group], Phys. Lett. B **592** (2004) 1; and 2005 update at <http://pdg.lbl.gov/>.
- [10] P.H. Frampton, P.Q. Hung and M. Sher, Phys. Rept. **330**, 263 (2000); J. I. Silva-Marcos, JHEP **0212**, 036 (2002);
- [11] W.S. Hou and A. Soddu, hep-ph/0512278.
- [12] K. M. Belotsky, M. Y. Khlopov, K. I. Shibaev, D. Fargion and R. V. Konoplich, Grav. Cosmol. **11** (2005) 16. D. Fargion, Y. A. Golubkov, M. Y. Khlopov, R. V. Konoplich and R. Mignani, Pisma Zh. Eksp. Teor. Fiz. **69**, 402 (1999) [JETP Lett. **69**, 434 (1999)]. S. Godfrey and S. h. Zhu, hep-ph/0405006.
- [13] A. de Gouvea, Phys. Rev. D **72**, 033005 (2005).
- [14] A. Aguilar *et al.* [LSND Collaboration], Phys. Rev. D **64**, 112007 (2001).
- [15] The final results from LEP on electroweak precision physics give [16]: $S = +0.07 \pm 0.10$, $T = +0.13 \pm 0.10$ (with U fixed at 0) for $m_H = 114$ GeV. At first sight this may seem to be more than 1σ shift for both S and T from 2003 data. However, taking additional factors into account, such as developments on top mass and low energy data, J. Erler [17] has reported that S and T are again negative, and the case against the 4th generation is even more stringent than stated in Ref. [9].
- [16] The ALEPH, DELPHI, L3, OPAL, SLD Collaborations, hep-ex/0509008, accepted to Phys. Rept.
- [17] J. Erler, hep-ph/0604035.
- [18] H.J. He, N. Polonsky and S.f. Su, Phys. Rev. D **64**, 053004 (2001); V.A. Novikov, L.B. Okun, A.N. Rozanov and M.I. Vysotsky, Phys. Lett. B **529**, 111 (2002).
- [19] Y. Chao *et al.* [Belle Collab.], Phys. Rev. Lett. **93**, 191802 (2004); B. Aubert *et al.* [BaBar Collab.], *ibid.* **94**, 181802 (2005).
- [20] W.S. Hou, M. Nagashima and A. Soddu, Phys. Rev. Lett. **95**, 141601 (2005).
- [21] See the webpage <http://www.slac.stanford.edu/xorg/hfag/> of the Heavy Flavor Averaging Group [HFAG].
- [22] W.S. Hou, M. Nagashima, G. Raz and A. Soddu, hep-ph/0603097.
- [23] A. Arhrib and W.S. Hou, Eur. Phys. J. C **27**, 555 (2003).

- [24] A more stringent result from recent kaon decay data gives $1 - |V_{ud}|^2 - |V_{us}|^2 = 0.0004 \pm 0.0011$ ($|V_{ub}|^2$ is negligible), or $|V_{ub}| < 0.047$ at 90% C.L. See E. Blucher, plenary talk at the XXII Lepton-Photon Symposium, June 2005, Uppsala, Sweden.
- [25] P. Abreu *et al.* [DELPHI Collaboration], Nucl. Phys. B **367**, 511 (1991).
- [26] S. Abachi *et al.* [D0 Collaboration], Phys. Rev. D **52**, 4877 (1995).
- [27] S. Abachi *et al.* [D0 Collaboration], Phys. Rev. Lett. **78**, 3818 (1997).
- [28] T. Affolder *et al.* [CDF Collaboration], Phys. Rev. Lett. **84**, 835 (2000).
- [29] F. Abe *et al.* [The CDF Collaboration], Phys. Rev. D **58**, 051102 (1998).
- [30] D. Acosta *et al.* [CDF Collaboration], Phys. Rev. Lett. **90**, 131801 (2003).
- [31] A. Arhrib and W.S. Hou, Phys. Rev. D **64**, 073016 (2001).
- [32] S.M. Oliveira and R. Santos, Phys. Rev. D **68**, 093012 (2003).
- [33] M.S. Chanowitz, M.A. Furman and I. Hinchliffe, Phys. Lett. B **78**, 285 (1978); Nucl. Phys. B **153**, 402 (1979).
- [34] T. Yanir, JHEP **0206**, 044 (2002).
- [35] W.S. Hou, M. Nagashima and A. Soddu, Phys. Rev. D **72**, 115007 (2005).
- [36] W. S. Hou, A. Soni and H. Steger, Phys. Lett. B **192**, 441 (1987).
- [37] W. S. Hou, R. S. Willey and A. Soni, Phys. Rev. Lett. **58**, 1608 (1987) [Erratum-ibid. **60**, 2337 (1988)].
- [38] J. Kaneko *et al.* [Belle Collaboration], Phys. Rev. Lett. **90**, 021801 (2003); K. Abe *et al.* [Belle Collaboration], hep-ex/0408119.
- [39] B. Aubert *et al.* [BABAR Collaboration], Phys. Rev. Lett. **93**, 081802 (2004).
- [40] G. Raz, Phys. Rev. D **66**, 057502 (2002).
- [41] T. Hattori, T. Hasuike and S. Wakaizumi, Phys. Rev. D **60**, 113008 (1999).
- [42] F.J. Botella and L.L. Chau, Phys. Lett. B **168**, 97 (1986). See also Ref. [36].
- [43] T. Hahn, Comput. Phys. Commun. **140**, 418 (2001); T. Hahn, C. Schappacher, Comput. Phys. Commun. **143**, 54 (2002); T. Hahn, M. Perez-Victoria, Comput. Phys. Commun. **118**, 153 (1999); T. Hahn, Nucl. Phys. Proc. Suppl. **135**, 333 (2004); J. Küblbeck, M. Böhm, A. Denner, Comput. Phys. Commun. **60**, 165 (1990); see T. Hahn: <http://www.feynarts.de>
- [44] G.J. van Oldenborgh, Comput. Phys. Commun. **66**, 1 (1991);

- [45] T. Hahn, Acta Phys. Polon. B **30**, 3469 (1999); T. Hahn and M. Rauch, hep-ph/0601248.
- [46] W.S. Hou and R.G. Stuart, Phys. Rev. D **43**, 3669 (1991). Phys. Lett. B **233**, 485 (1989).
- [47] W.S. Hou and R. G. Stuart, Nucl. Phys. B **349**, 91 (1991).
- [48] W. S. Hou and R. G. Stuart, Phys. Rev. Lett. **62**, 617 (1989); Nucl. Phys. B **320**, 277 (1989).
- [49] B. Haeri, A. Soni and G. Eilam, Phys. Rev. Lett. **62**, 719 (1989); *ibid* Phys. Rev. D **41**, 875 (1990).
- [50] I.I. Y. Bigi, Y.L. Dokshitzer, V.A. Khoze, J.H. Kühn and P. M. Zerwas, Phys. Lett. B **181**, 157 (1986).
- [51] D. Atwood, L. Reina and A. Soni, Phys. Rev. D **53**, 1199 (1996); J. j. Cao, G. l. Liu and J. M. Yang, Eur. Phys. J. C **41**, 381 (2005).
- [52] D. Atwood, L. Reina and A. Soni, Phys. Rev. Lett. **75**, 3800 (1995).
- [53] A. Arhrib, Phys. Rev. D **72**, 075016 (2005).
- [54] S. Bar-Shalom, G. Eilam, A. Soni and J. Wudka, Phys. Rev. D **57**, 2957 (1998).
- [55] W.S. Hou, G.L. Lin and C.Y. Ma, Phys. Rev. D **56**, 7434 (1997).
- [56] D. Atwood, S. Bar-Shalom, G. Eilam and A. Soni, Phys. Rev. D **66**, 093005 (2002); B. Grzadkowski, J.F. Gunion and P. Krawczyk, Phys. Lett. B **268**, 106 (1991); B. Mukhopadhyaya and A. Raychaudhuri, Phys. Rev. D **39**, 280 (1989); M.J. Duncan, Phys. Rev. D **31**, 1139 (1985).
- [57] W.S. Hou and R.G. Stuart, Phys. Lett. B **226**, 122 (1989).
- [58] C.S. Huang, X.H. Wu and S.H. Zhu, Phys. Lett. B **452**, 143 (1999).
- [59] C.S. Huang, X.H. Wu and S.H. Zhu, J. Phys. G **25** (1999) 2215.
- [60] $V_{t'd}$ and $V_{ub'}$ cannot both vanish, but for purpose of b' and t' search, ignoring them is a valid approximation for practical purposes.
- [61] See e.g. M. Beneke, Phys. Lett. B **620**, 143 (2005).